Evaluating interface properties of geomembrane and compacted clay liners for landfill liner stability

Saravanan, M.[1]. Kamon, M.[2], Faisal, H. A.[3], Katsumi T.[4], Akai, T.[5], Inui, T.[6], and Matsumoto, A.[5]

[1] *Graduate Student, Graduate School of Global Environmental Studies, Kyoto University, Kyoto, Japan*

[2]*Professor, Graduate School of Global Environmental Studies, Kyoto University, Kyoto, Japan*

[3]*Professor, Department of Civil Engineering, University Malaya, Kuala Lumpur, Malaysia.*

[4]*Associate Professor, Graduate School of Global Environmental Studies, Kyoto University, Kyoto, Japan*

[5]*Senior Research Scientist, Technology Research Institute of Osaka Prefecture, Osaka, Japan*

[6]*Assistant Professor, Graduate School of Global Environmental Studies, Kyoto University, Kyoto, Japan*

ABSTRACT: Majority of failure occurs within waste mass and along landfill liners. This paper will discuss the methods adopted to study landfill liner interface performances. Interfaces shear strength parameter evaluation for landfill liner systems have been a tedious testing process. Various testing methods and guidelines have been proposed by engineers and researchers over the years. The current testing procedures are based on ASTM testing guideline and basic fundamental engineering testing philosophies. Hence there is a need for much ideal testing equipment which can perform the entire test series required for landfill liner parameter evaluations. The equipment are required to perform interface test between 1) soil and soil (CCLs), 2) geomembrane (HDPEs and PVC) and soil, 3) geosynthetic (GCLs) / compacted clay liners (CCLs) and soil, 4) geomembrane and geotextile, 5) geotextile and soil, 6) geotextile and geosynthetic (GCLs) / compacted clay liners (CCLs), 7) geomembrane and geosynthetic (GCLs) / compacted clay liners (CCLs). Having such variety in requirement and testing complexity for landfill liner system, this paper also addresses the modification made to a large scale shear box in order to perform the above said interface tests. The shear box is modified to perform interface test under wet condition and at optimum condition. However data of optimum conditions are presented herewith. The modified large scale shear box is used to study interface performance of various combination of liners. Two common type of compacted clay liners (CCLs), which are silt bentonite mixture (100 : 10) and sand bentonite mixture (100 : 10), studied together with geomembrane. The interface parameter data are then compiled to be a quick reference guide for engineers.

1 INTRODUCTION

The world consumption of natural resources has been increasing exponentially. In Japan the consumption of resource is at 1900 million tones annually. This consumption generates waste of 600 million tones, which consist of 400 million tons of industrial waste and 50 million tons of municipal waste. Out of this 220 million tons are recycled and reused, 324 million tons are pre-treated waste for disposal. 56 million tons are disposed to landfill in Japan in year 2000. The estimated operational period of landfill site in Japan is about 6 to 10 years. It becomes very difficult to build new sites in Japan due of the syndrome of "Not In My Back Yard". The cost of new site in Tokyo could cost up to 500 million US dollars. The running cost of existing landfill site in Tokyo is at about 300 USD / m^3.

A landfill also behaves as in-situ bioreactor, where the contents undergo complex biochemical reactions. The adoption of suitable design and construction methods are essential not only to reduce design and construction cost, but also to minimize long term operation, maintenance and monitoring cost.

1.1 Basic landfill design

An engineered landfill site must be geologically, hydrologically and environmentally suitable. As such landfill site need to be carefully design to envelope the waste and prevent escape of leachate into the environment. Most important requirement of landfill site is that it does not pollute or degrade the surrounding environment.

An engineered Municipal Solid Waste landfills consist of the following (Xuede Qian (2002):

i. Bottom and lateral side liners system
ii. Leachate collection and removal system
iii. Gas collection and control system

iv. Final cover system
v. Strom water management system
vi. Ground water monitoring system
vii. Gas monitoring system

During construction or design of a landfill site, the engineers required to perform detail engineering evaluation on :

i. Landfill foot print layout
ii. Subsoil grading
iii. Cell layout and filling
iv. Temporary cover selection
v. Final cover grading
vi. Final cover selection

The above are directly relate to geotechnical engineering works which involves the use of ground improvement and slope stabilization technology. Although the issue of landfill and environmental stability is part of global environmental problem, it is essential to solve them one by one. Every geotechnical engineers are required to engage in the environmental engineering problems with the motto of "Think Globally, Act Locally" (Kamon 2001).

2 LANDFILL STABILITY

Stability of landfills has been a major concern of the present environmental geotechnical engineering community. Failures at landfill sites can be minor, however the cost of rectification is huge. As landfill sites generally used to contain solid waste of various kinds, which some can contaminate and harm the environment. Hence landfill failures could lead to serious environment pollutions. However, stability is an issue that has be sometimes overlooked for the need of maximization of waste storage per unit area during continuous filling exceeding the initially design. In general majority of landfill sites are overfilled. Cincinnati landfill is an example of failure caused by overfilling and rapid expansion (Timoth, 2000). Koerner and Soong (2000b) presented and analyzed ten large solid waste landfill failures, including Kettleman, Cincinnati and some of the world landfill failures. The ten solid waste failure can be generally characterized into (Wenxing Jian 2001);

i. Wide range failure in their geographic distribution
ii. Extremely large in volume and lateral movement
iii. Rapid and generally unexpected
iv. Associated with excessive amounts of liquids (over, under or within the liner system); to the point where liquefication takes place.
v. Involving extensive remediation which sometime include insurance and litigation cost

Table 2 : Summary of waste failures (Koerner and Soong, 2000)

Case History	**Location**	**Type of Failure**	**Quantity Involved**
(Unlined Sites)			
U-1 - 1984	North America	Single Rotational	110,000 m^3
U-2 - 1989	North America	Multiple Rotational	500,000 m^3
U-3 - 1993	Europe	Translational	470,000 m^3
U-4 - 1996	North America	Translational	1,100,000 m^3
U-5 - 1997	North America	Single Rotational	100,000 m^3
(Lined Sites)			
L-1 - 1988	North America	Translational	490,000 m^3
L-2 - 1994	Europe	Translational	60,000 m^3
L-3 - 1997	North America	Translational	100,000 m^3
L-4 - 1997	Africa	Translational	300,000 m^3
L-5 - 1997	North America	Translational	1,200,000 m^3

The failure commonly occurs along liner slope, through landfill foundations, surface side slope and within the waste mass itself. In addition to such failures, failures have also occurred during cell excavation, liner system construction, waste filling and after landfill closure. All of it is classical geotechnical mode of failure depending upon site specific conditions, the placement and geometry of the waste mass (Xuede Qian, 2003). Potential failure mode include the following ;

i. Sliding failure along the leachate collection system
ii. Rotational failure along sidewall slope and base
iii. Rotational failure through waste, liner and foundation subsoil
iv. Rotational failure within the waste mass
v. Translational failure by movement along the underlying liner system

The failures through liner system beneath the waste mass are common, cause by multiple layer components consist of clay, soils and geosynthetic materials. Double-lined system can consist of as many as 6 to 10 individual components. As such

the interfaces resistance of the individual components against shear stress could be low and cause potential failure plane. Figure 1 and 2 shows the type of potential failure along the liner system.

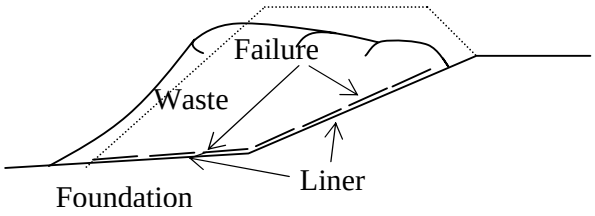

Figure 1 : Failure Completely Along (or Within) Liner System (Xuede Qian, 2003)

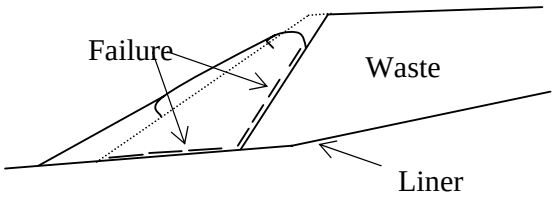

Figure 2 : Failure Along (or Within) Liner System and Solid Waste (Xuede Qian, 2003)

The liners and closure cover system of a modern MSW landfill are constructed with layers of material having dissimilar properties, such as compacted clay or geosynthetic clay liner, geomembrane (liquid barrier), geonet (drainage layer), geotextile (filter) and geogrid (reinforcement). Typical detail of such system is shown in Figure 3. While compacted clay or geosynthetic clay and geomembranes function effectively as flow barriers to leachate and infiltration, their interface peak and residual friction angles are lower than those of the soil alone. Such lower friction angle between a geomembrane and other geosynthetics could trigger much rapid failure during seismic loading conditions.

The soil-geomembrane interface acts as a possible plane of potential instability of the system under both static and seismic loading (Hoe I. Ling, 1997). Hence environmental geotechnical engineers are very concern about the potential instability caused by the waste containment liner system. Attention to slope stability of municipal solid waste during static and seismic loading has increased following report of Kettleman Hills waste landfill failure. The cause of failure was due to low friction angle between the soil and geosynthetic or geosynthetic layers in the liner system. This failure however was not attributed to seismic loading. Seismic performance of landfills has been reported for the 1989 Loma Prieta Earthquake and the 1994 Northridge Earthquake. Seismic design of landfill systems should include response analysis, liquefaction analysis, deformation analysis and slope stability analysis. Shear failure involving liner system can occur at three possible location :

i. The external interface between top of liner system and the overlying material
ii. Internally within the liner system
iii. Interface between clay liner and geosynthetic layer
iv. The external interface between the bottom of the liner system and the underlying subsoil material

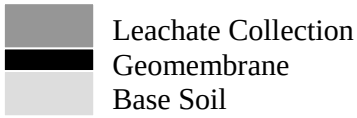

(a) Single geomembrane liner

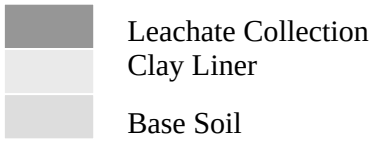

(b) Single clay liner

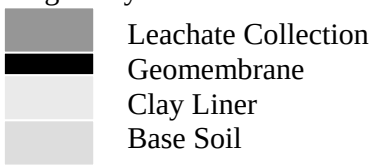

(c) Single composite liner

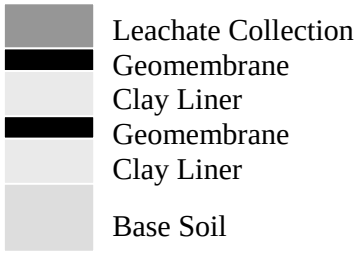

(d) Double liner

Figure 3 : Cross section of typical bottom liner systems (Kamon, 2001)

Current engineering design practice is to establish appropriate internal and interface shear strength parameters for design using direct shear test on test specimens and employing traditional limit equilibrium techniques for analyzing the landfill slope stability (David E. Daniel, 1998). As such simplified Janbu analysis procedure is recommended as it often gives factor of safety that is significantly less than those calculated by Spencer's procedure (Robert B. Gilbert, 1998).

2 LANDFILL STABILIY RESEARCH

The above discussion calls for detail and compressive study of landfill stability on the following :

a. Study landfill liner components and their physical properties
b. Study the compacted clay liner (CCLs) interface properties with geomembrane and geosynthetic clay liners (GCLs).
c. Study the interface properties of compacted clay liners (CCLs) with native soils
d. Study the interface properties between CCL, GCL, non woven geotextile and geomembrane.
e. Study the suitable configuration of composite liner system which could improve the liner stability without neglecting the hydraulic conductivity requirement

In order to conduct the above said study careful selection of test materials and configuration of liner system were used in the research.

2.1 Landfill liner configuration

The list of interface test conducted will dependent on the configuration and material used for landfill liner system, adopted for research. The liner configuration used for research is shown in Figure 4. The research configuration consists of both single and double composite liner system. The research is still under progress to study the interface performance under wet condition for both single and double composite liner system. Nine type of liner configurations were studied in the research. The configuration consists of two type of single membrane liner and seven type of single composite liner. Details and description of the said liner configuration are listed and discussed under results and discussion. The details of selected materials are as follows:

i. Mountain sand was used as sand
ii. Non Woven Geotextile of 10mm thick
iii. Geomembrane
   a. HDPE Geomembrane
      - Type 1 – Smooth non textured
      - Type 2 – Textured membrane (blown-film texturing)
   b. PVC Geomembrane
      - rough rear side
      - smooth front side

iv. Compacted Clay Liners (CCLs)
   a. Silt and Bentonite Mix (100 : 10)
   b. Sand and Bentonite Mix (100 : 10)

v. Geosynthetic Clay Liner (GCL)
   - GCL Type 1 – Adhesive-bond bentonite to geomembrane (wavy textured)

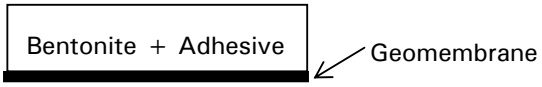

   - GCL Type 2 – Stitch bonded non woven geotextile and woven geotextile sandwiching bentonite

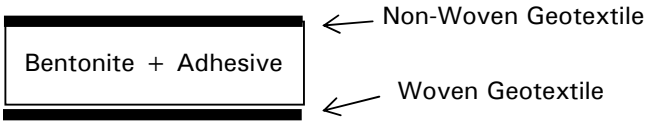

vi. Native Soil type - Decomposed granite soil

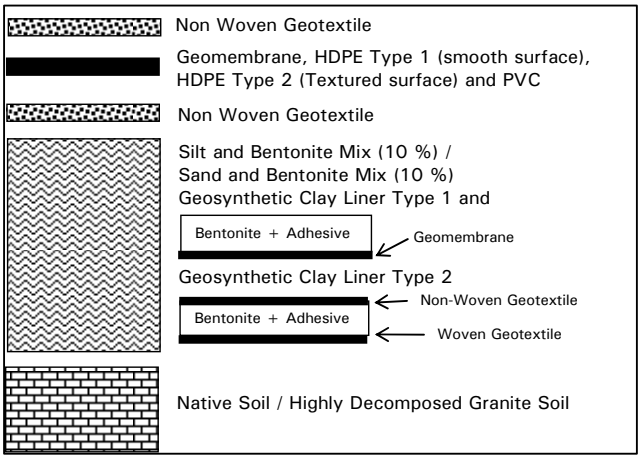

Figure 4 : Simplified configuration for interface research

Smooth and textured geomembranes were studied to validate the interface properties due to plowing and frictional contribution of textured surface as compared to smooth surface. Where the measured friction coefficient for smooth particles is relatively low and plowing is not an important contributor. Whereas rougher and more angular particles have relatively larger friction coefficients and plowing is important even at low normal loads. (Joseph E. Dove, 1999). In order to conduct the listed interface tests modifications were made to large scale shear box. The shearing machine was modified to provide maximum normal load of 300 kPa and constant shearing speed of 1 mm/min with maximum shearing displacement of 100mm. Each interface tests were tested for normal loads of 100,

200 and 300 kPa to obtain interface properties. Clamping mechanism was introduced to hold the geosynthetic in place during shearing. Modifications were also done to introduce pore pressure transducers to measure pore pressures during shearing under saturated condition. However this paper discusses test data from as installed condition only.

2 SHEAR BOX MODIFICATION

The modifications of large scale shear box for interface shear strength evaluation for landfill liners were developed based on the guideline of

i. American Standard – ASTM D3080 – 98 – Standard Test Method for Direct Shear Test of Soils Under Consolidated Drained Conditions.
ii. American Standard – ASTM D5321 – 02 – Standard Test Method for Determining the Coefficient of Soil and Geosynthetic or Geosynthetic and Geosynthetic Friction by the Direct Shear Method.
iii. American Standard – ASTM D6243 – 98 – Standard Test Method for Determining the Internal and Interface Shear Resistance of Geosynthetic Clay Liner by the Direct Shear Method.

As per the ASTM guideline and testing requirement the apparatus design is subdivided into three categories, namely

i. Soil and soil internal and interface testing to perform test on
   - Interface shear strength between native soil and compacted clay liners.
   - Internal shear strength of native soil and compacted clay liners.
ii. Geosynthetic and geomembrane interface testing to perform test on
   - Geomembranes and geotextile
   - Geotextile and geosynthetic clay liners
   - Geomembranes and geosynthetic clay liners
iii. Geosynthetic and soil interface testing to perform test on
   - Geomembranes and native soil / compacted clay liners
   - Geotextile and native soil / compacted clay liner

Following are the design guide adopted to modify the large scale shear box

i Shear box design adaptation

a. The shear box size shall have minimum size of 300mm x 300mm or 15 times the d_{85} of the coarse soil sample used, or 5 times the maximum opening size (in plan) of the geosynthetic to be tested. The adopted shear box size was 250mm x 500mm for top box and 300mm x 600mm for bottom box.
b. The shear box height shall have a minimum height of 50mm or 6 times the maximum particle size of the coarse soil used. The adopted box height ranges between 75mm for bottom box and 100mm for top box.
c. Test failure is defined as shear stress at 15 % to 20 % of relative lateral displacement. The shear machine was modified to have maximum displacement of 100mm which is 20 % of 500mm of top shear box length.
d. The box is required to be made of stainless steel with sufficient thickness to avoid box deformation during loading and shearing. Hence box thickness of 12mm was adopted.
e. The top and bottom box opening shall be ½ of d_{85} or 1mm.

ii. Geosynthetic (Geosynthetic Clay Liner, Geotextile and Geomembrane) clamping method adopted

a. Flat jaw like clamping device and rough surface were used to grip the geosynthetics
b. The gripping jaw and rough surface were firm enough to allow geosynthetic outer surface being sheared while the inner side remained gripped firmly.
c. The gripping surface completely transfers the shear stress through the outside surface into the geosynthetic.
d. The gripping was modified not to damage the geosynthetic and not to influence the shear strength behavior of the geosynthetic.
e. Rough surface was introduced by using high strength double sided tape. The tapes provide strong gripping force without damaging the geosynthetic.
f. The rough surface was to simulate frictional resistance from adjacent liner components.

g. The failure surface was entirely within the geosynthetic member.
h. The geosynthetic was free to displace in the direction of shear allowing geosynthetic to mobilize the tensile forces beyond the base rough surface resistance.
i. This clamping method allows geosynthetics to mobilize tensile forces during large displacement.

iii. Shearing Process adopted

a. The shearing machine was required to have displacement rate of 0.025mm/min to 6.35mm/min however the machine was tuned to adopt constant displacement rate of 1mm/min. Displacement rate have relatively small effect on measured shear strength, (Patrick J. Fox, 1998).
b. The normal loading was applied using air bag system within fix frame. Due to this vertical displacements were restricted from taking place.
c. The load cell or proving ring have an accuracy of 2.5N to record and monitor shearing forces.
d. Horizontal displacement measuring device has an accuracy of 0.02mm with maximum displacement of 110mm.
e. LVDT – Linear Variable Differential Transformer was used to measure displacements.

The above listed was the summary of interface and internal shear strength test requirement and modification adopted base on the guideline in , ASTM D3080-98, ASTM D5321-02 and ASTM D6343-98. With such stringent guide and testing complexity, much attention was paid to modify the conventional shear box to compile the standard guideline. The shear box was also modified to record pore pressure readings under wet condition. However data were not presented herewith as the research is in progress. Figures 6a, b, c, 7a, b, c and 8a, b, c shows some of the typical modifications of large scale shear box adopted for the research work for three different test conditions. Namely i) Case 1 – Interface testing between geosynthetic and geosynthetic, ii) Case 2 - Interface testing between geosynthetic and soil, and iii) Case 3 - Interface testing between soil and soil. Bottom shear box size of 350 x 600mm and top box size of 250 x 500mm were used for the test. Larger 100mm bottom box in shearing direction was used to define test failure of 15 % to 20% to relative lateral displacement of the top box dimension. The larger bottom box was adopted in order to provide additional rough surface for gripping forces on to geosynthetic during shearing. The shearing surface contact areas were made same for both top and bottom box of 250 x 500mm in size allowing control and specific shearing area with reduction in contact area during shearing. Height adjustable bottom box base plate with spacer blocks were introduced to cater for variation in sample thickness and allowance for settlement or sample deformation during normal loading prior to shearing. The spacer blocks minimize plowing kind of effect during shearing process, occurring when two different material hardness are in contact and sheared. Due to area reduction during shearing, area correction method was adopted to obtain shear stresses. Constant shearing speed of 1 mm/min was used for test normal loads of 100, 200 and 300 kPa for the interface tests.

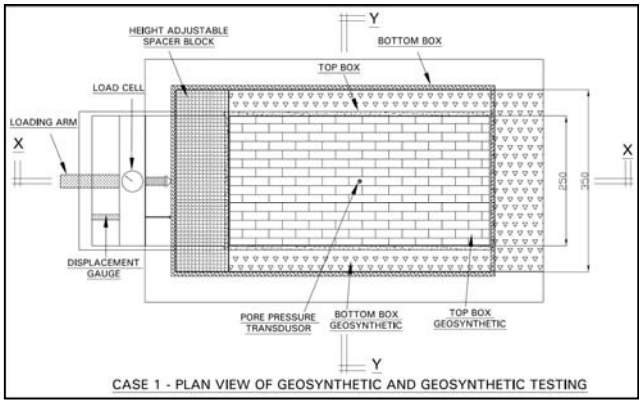

Fig. 6a : Case 1 – Modification adopted for geosynthetic and geosynthetic testing – Plan view

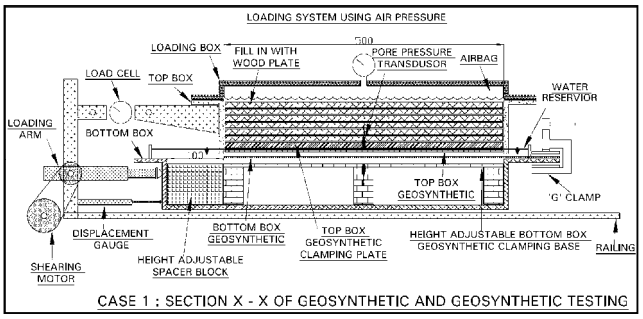

Fig. 6b : Case 1 – Modification adopted for geosynthetic and geosynthetic testing – Section X-X

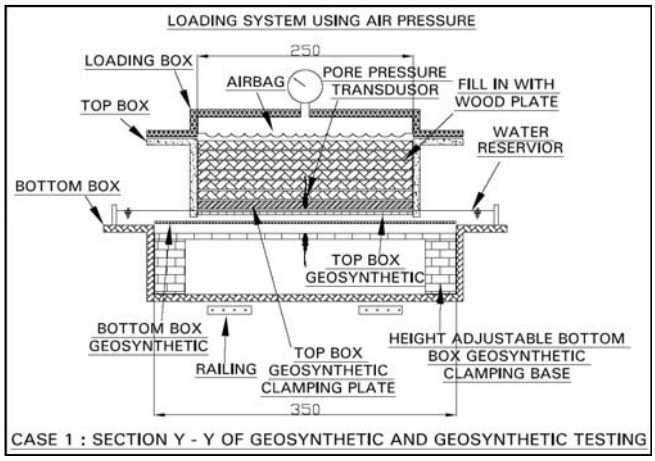

Fig. 6c : Case 1 – Modification adopted for geosynthetic and geosynthetic testing – Section Y-Y

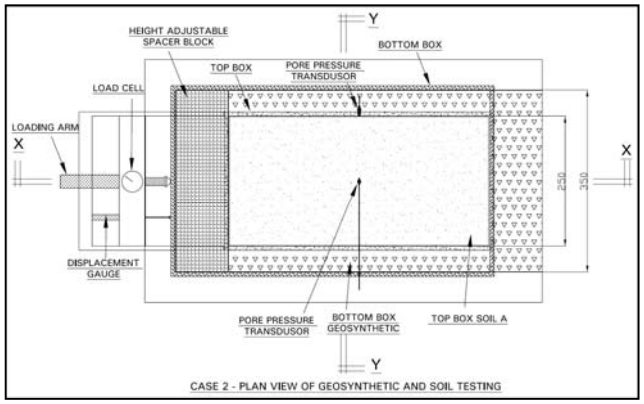

Fig. 7a : Case 2 – Modification adopted for geosynthetic and soil testing – Plan view

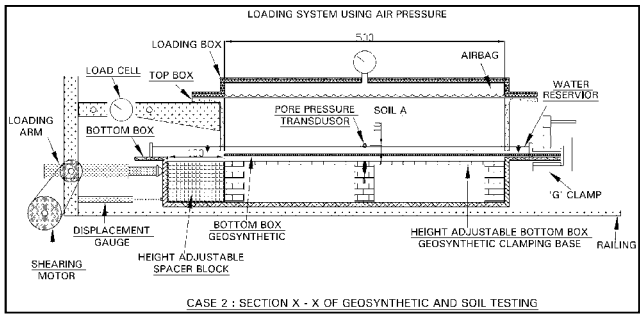

Fig. 7b : Case 2 – Modification adopted for geosynthetic and soil testing – Section X-X

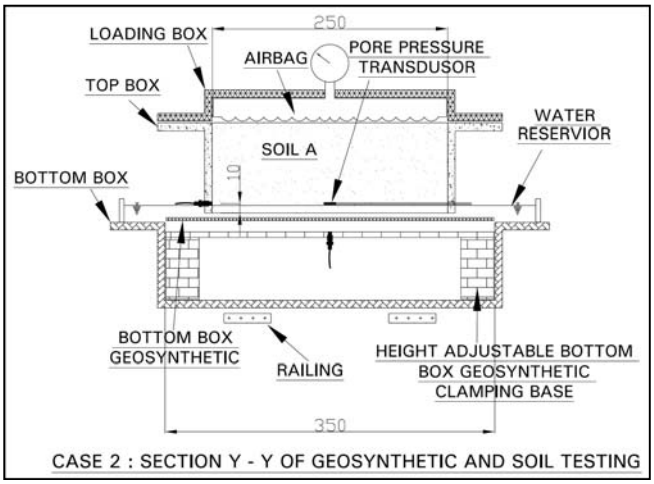

Fig. 7c : Case 2 – Modification adopted for geosynthetic and soil testing – Section Y-Y

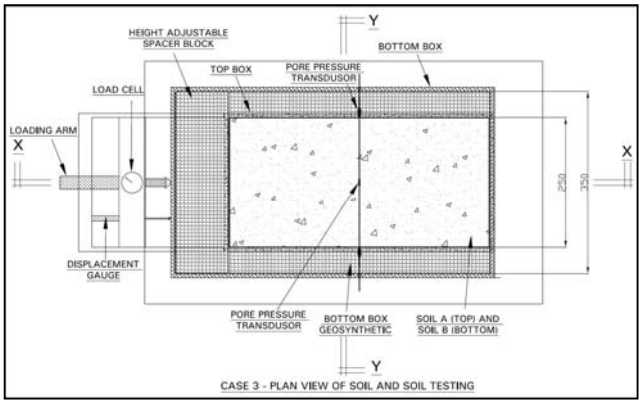

Fig. 8a : Case 3 – Modification adopted for soil and soil testing – Plan view

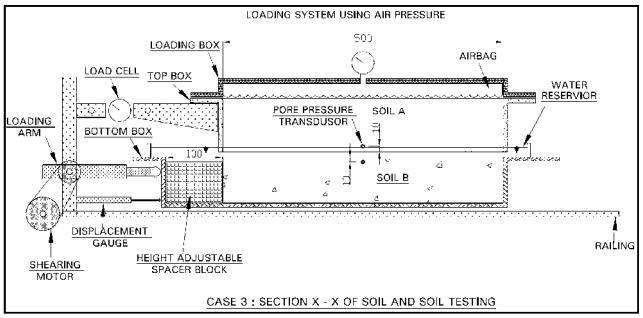

Fig. 8b : Case 3 – Modification adopted for soil and soil testing – Section X-X

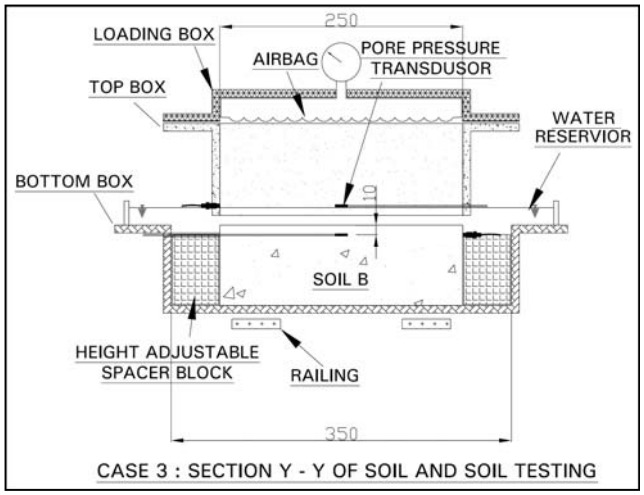

Fig. 8c : Case 3 – Modification adopted for soil and soil testing – Section Y-Y

3 TEST MATERIAL PHYSICAL PROPERTIES

The selected properties are tested for their basic physical properties such as tensile strength, elongation, cohesion, friction, permeability, etc. Details of material properties are presented as follows.

1. Geosynthetics comprise of non woven geotextile, HDPE Type 1 (smooth surface), HDPE Type 2 (textured surface) and PVC geomembranes.

Table 3 : Summary of geosynthetic physical properties

Description	Geotextile	PVC	HDPE – Type 1 and 2
Thickness	10mm	1.5 mm	1.5 mm
Tensile strength	160 N/cm (Weft) 80 N/cm (Wrap)	300 N/cm both Weft and Wrap	544 N / cm both Weft and Wrap
Elongation at break	70 N/cm (Weft) 55 N/cm (Wrap)	320 % both Weft and Wrap	790 % both Weft and Wrap

The details of tensile strength test results are presented in figures 9a and 9b for both warp and weft direction respectively for geosynthetics.

2. Geosynthetic Clay Liners comprise of 1) type 1 – adhesive bond bentonite to geomembrane and 2) type 2 – stitch bonded non woven goetextile and woven goetextile sandwiching bentonite.

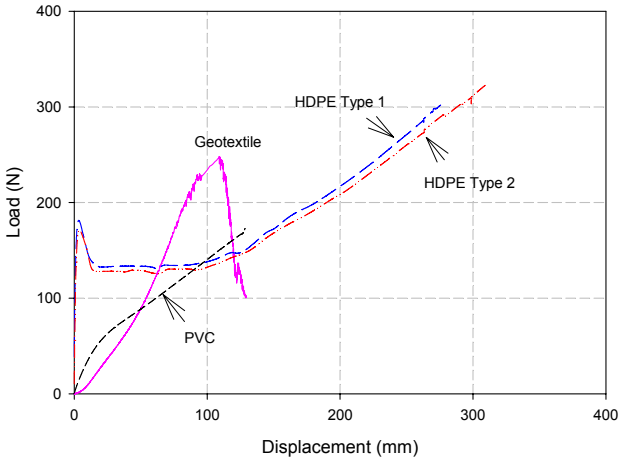

Figure 9a : Geosynthetic tensile strength plot on warp direction

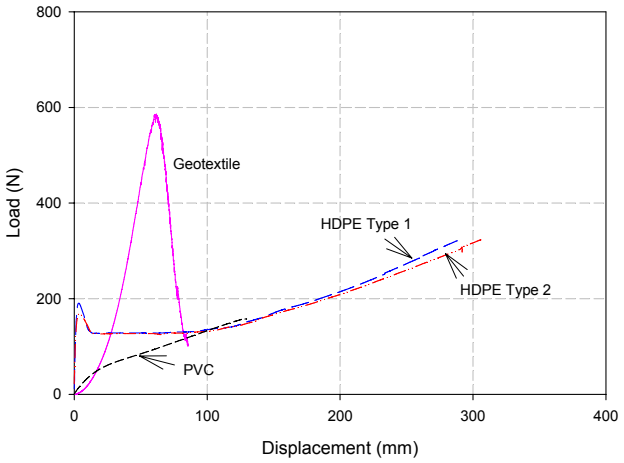

Figure 9b : Geosynthetic tensile strength plot on weft direction

3. Compacted Clay Liners comprise of 1) silt bentonite mixture of 100 to 10 percent ratio and 2) sand bentonite mixture of 100 to 10 percent ratio. Native soil was from highly weathered granitic soil origin.

Shear box tests were done using small shear box of 60mm x 60mm with constant shearing speed of 1 mm/ min. The results represent total cohesion and friction parameters. Sand and silt mixed with bentonite shows similar friction, however sand mixture had higher cohesion contribution. As for granitic soil the contribution of both cohesion and frictional were sufficient to provide strong founding base. With the parameters obtained probability of internal failures of sand or silt bentonite mixture are less as compared to probability of interface failures within liner configurations.

Table 4 : Summary of Geosynthetic Clay Liner (GCL) physical properties

Description	GCL Type 1	GCL Type 2	Composite of GCL Type 2
Thickness - Bentonite - HDPE - Non Woven geotextile - Woven geotextile	 ?? mm ?? mm	 ?? mm ?? mm	 ?? mm ?? mm
Tensile strength - HDPE - Non Woven geotextile - Woven geotextile	 ?? N/cm	 ?? N/cm ?? N/cm	 ?? N/cm
Elongation at break - HDPE - Non Woven geotextile - Woven geotextile	 ?? %	 ?? % ?? %	 ?? %

Table 5 : Summary of CCLs and native soil properties

TEST USING CASAGRANDE		SAND BENTONITE (100 : 10)	SILT BENTONITE (100 : 10)	GRANITIC SOIL
Liquid limit, LL ,w_L	%	47	69	-
Plastic limit, PL, w_P	%	23	35	-
Plasticity Index,PI, Ip		23	34	-
Average Particle Density, ρ_s	Mg / m^3	2.60	2.64	2.59
Dry Density, ρ_d	Mg / m^3	1.9	1.68	2.06
Optimum Moisture Content, Mc	%	10.5	17.5	9
Classification		CL / OL ORGANIC SILT OR CLAY OF LOW PLASTICITY	CH / OH CLAY HIGH PLASTICITY	HIGHLY WEATHERED GRANITIC SOIL
SHEAR BOX TEST RESULTS				
C_u	kPa	77.0	43.1	31.4
Fi_u	o	34.3	35.8	45.5
CIU TEST RESULTS				
C'	kPa			
Fi'	o			
Permeability				

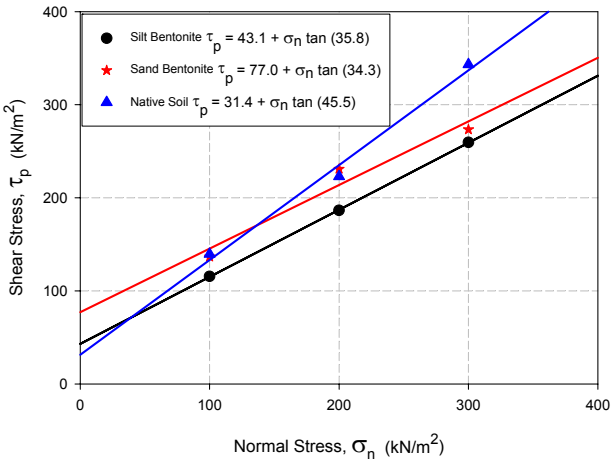

Figure 10 : Summary total shear stress parameters for internal failures of compacted clay liners and base material.

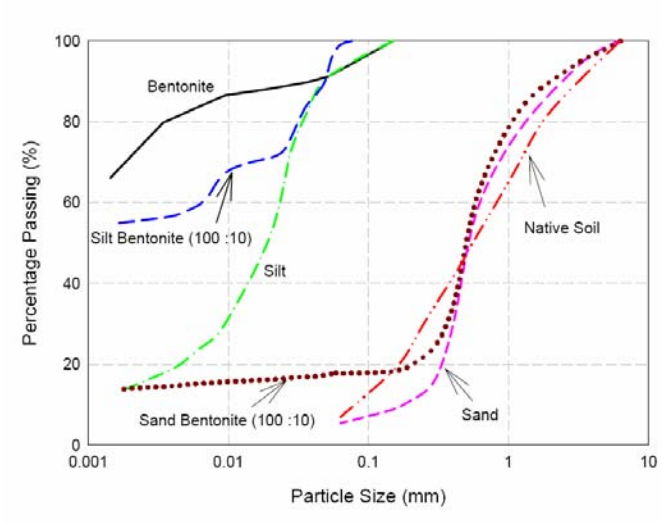

Figure 11 : Summary of classification plot

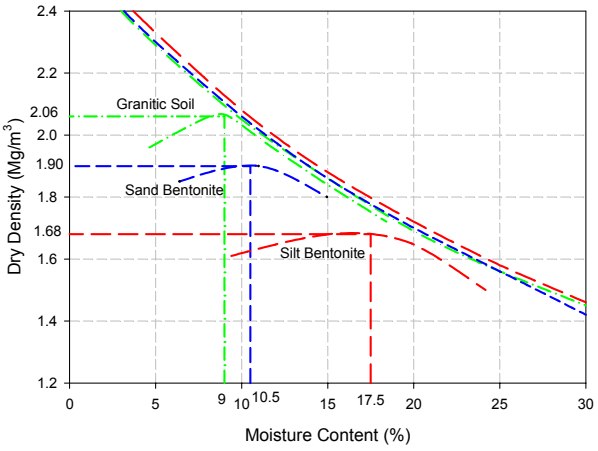

Figure 12 : Optimum dry density plot

Soil classification and dry density plots are shown in Figure 11 and 12 respectively. Silt bentonite mixture require optimum moisture content of 17.5 percent as compared to 10.5 and 9 percent for sand bentonite and native soil respectively to achieve maximum dry density. The compacting test was done using 4.5 kg, drop hammer. as per BS 1377 : Part 4 : 1990. For shear box compaction, hand held electric vibrating compaction machine was used with base size of 250 x 150 mm and 5kg in weigth. Careful calibration was done to obtain optimum compaction time required to achieve minimum compaction density of 90 percent for soil samples placed in the shear box. Five layer compaction with minimum 12 minutes compaction time per layer, was adopted to compact the soil samples into shear boxes. Figures 13 a, b, 14 a, b and 16 a, b shows the plot of moisture content, dry and bulk density and relative compaction density obtained for all interface tests carried out.

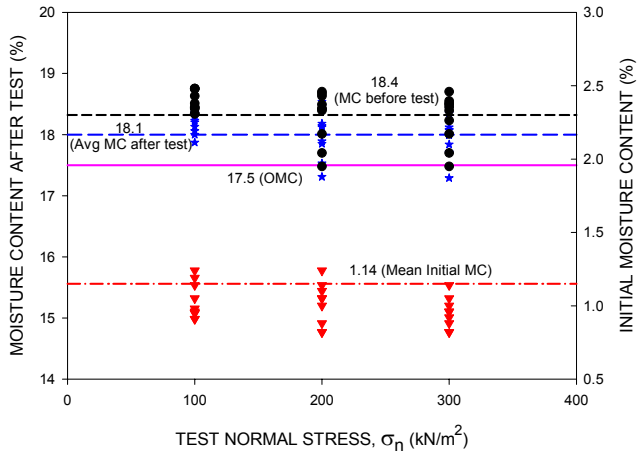

Figure 13a : Sample moisture content before and after test for Silt Bentonite mixture (100 : 10)

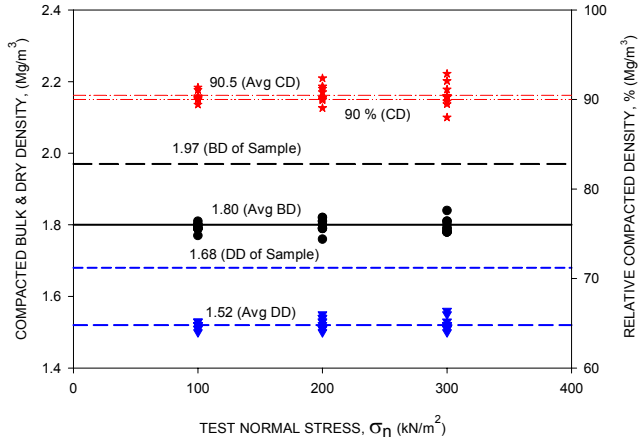

Figure 13b : Sample compacted bulk, dry density and compaction relative density for Silt Bentonite mixture (100 : 10)

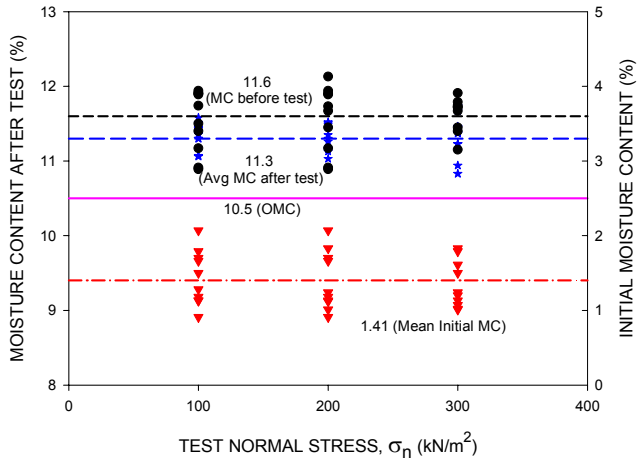

Figure 14a : Sample moisture content before and after test for Sand Bentonite mixture (100 : 10)

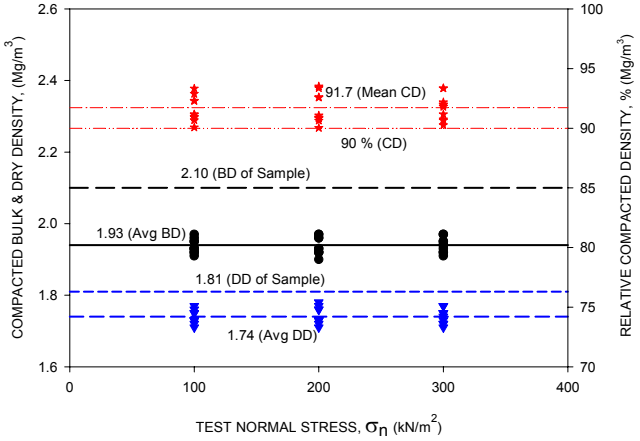

Figure 14b : Sample compacted bulk, dry density and compaction relative density for Sand Bentonite mixture (100 : 10)

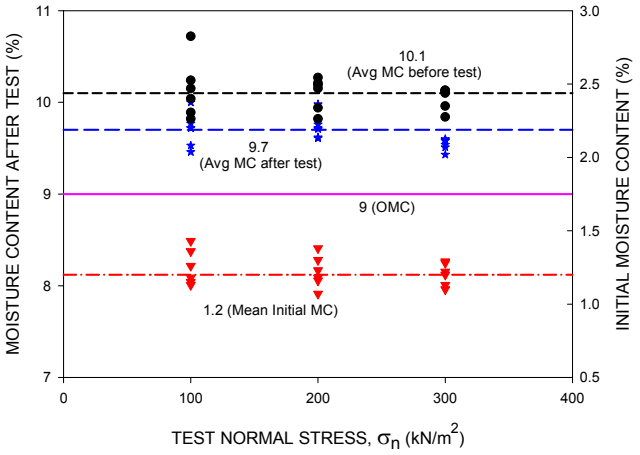

Figure 15a : Sample moisture content before and after test for Native soil

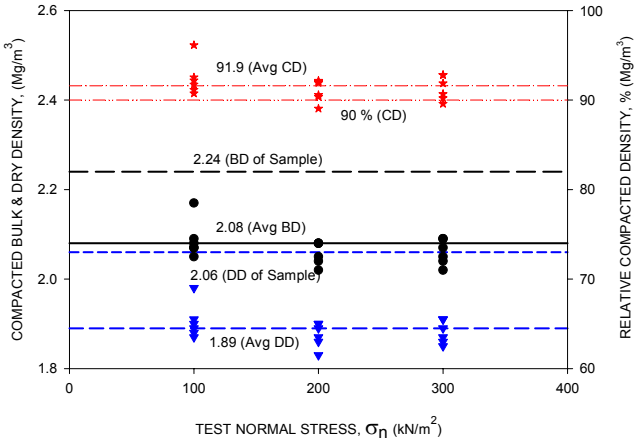

Figure 15b : Sample compacted bulk, dry density and compaction relative density for Native soil

5 INTERFACE TEST RESULTS

In order to obtain much clear understanding of interface test results, the test data are grouped into 8 categories. The categories were made by grouping one single member interfacing with others. The categories are

i. Geotextile interfacing with geomembrane, namely HDPE Type 1 and 2, PVC and GCLs Type 1 and 2
ii. HDPE Type 1 and 2 interfacing with PVC and GCLs Type 1 and 2
iii. PVC interfacing with GCLs Type 1 and 2
iv. Geosynthetic interfacing with CCLs – Silt Bentonite (100 : 10)
v. GCLs interfacing with CCLs – Silt Bentonite (100 : 10)
vi. Geosynthetic interfacing with CCLs – Sand Bentonite (100 : 10)
vii. GCLs interfacing with CCLs – Sand Bentonite (100 : 10)
viii. Geosynthetic interfacing with Native Soil (Highly weathered granitic soil)

The above interface test results indicate the presents of strain incompatibility between test members. The peak shear stresses were reached between 2 to 15 % strain. Hence the selections of peak stresses were limited to maximum stresses reached within 8% strain. Peak shear stresses were plotted with normal stresses to obtain peak failure envelope. Best fit liner plots were adopted in order to obtain total cohesion and total interface friction angle. The shear stress intersections were set to be either through axis or positive cohesion.

5.1 Geotextile interfacing with geomembrane and GCLs

Using peak shear stresses geotextile interfacing with PVC and GCL Type 1 (bentonite side), found to have high cohesion and frictional resistance. This could be due to plowing kind of effects created during shearing. The performance of HDPE was dominated by textured surface HDPE as predicted. The weakest was between geotextile and geotextile from GCL Type 2 and HDPE Type 1. Details of test results are presented in Table 5 and Figures 16a to 16i respectively. In Figure 16a it shows clearly that HDPE type 1 (smooth surface) stand out of the group. Hence designers should avoid direct interface between HDPE type 1, goetextile of both woven and non woven with geotextile.

Table 5 : Test results of geotextile interfacing with geomembrane

Test	Interface Parameters	Cohesion (kN/m^2)	Friction Angle (^{o})
Interface Parameters Between Geotextile and HDPE, PVC, GCLs			
Test 1A	GEOTEXTILE & HDPE Type 1	0.0	7.6
TEST 2A	GEOTEXTILE & HDPE Type 2	3.2	21.1
TEST 3A	GEOTEXTILE & PVC (Rear Side)	11.1	18.7
TEST 3C	GEOTEXTILE & PVC (Front Side)	25.7	17.1
TEST 4A	GEOTEXTILE & GCL Type 1 (Bentonite side)	12.1	17.1
TEST 4C	GEOTEXTILE & GCL Type 1 (HDPE Side)	0.0	21.8
TEST 5A	GEOTEXTILE & GCL Type 2 (Non Woven Site)	1.5	15.1
TEST 5C	GEOTEXTILE & GCL Type 2 (Woven Side)	10.5	14.8

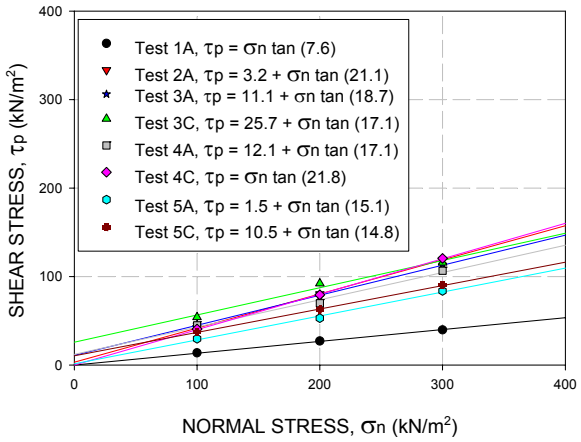

Figure 16a : Summary of peak failure envelopes for geotextile interfacing with geomembrane.

For geotextile and HDPE type 1 interface, the peak shear stresses were reached within strain of 1 to 1.5 % . Beyond peak stresses constant reduction in shear stresses were observed before constant increment in shear stresses in residual region. Continuous increments in shear stresses were observed beyond 10% strain in the residual region. The rate of residual shear stresses increment was relatively minor for lower normal stresses as compared to higher normal stresses. Hence in the case of geotextile and HDPE type 1 interface the residual shear stress increases gradually for lower normal stresses and increases rapidly for higher normal stresses beyond strain of 10%. No plowing kind of effects was observed in the test. Surface deformation was observed on HDPE type 1, where wavy stress marks were observed on the smooth HDPE surface. Higher concentrations of wavy stress marks were observed as the normal loads increased in the direction of shear. These wavy formations believed to be cause of increase in shear stresses in the residual region. Figure 16b shows

the shear stress plots for interface test between geotextile and HDPE type 1 – Test 1A.

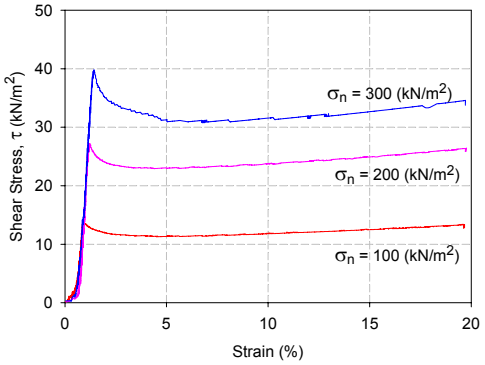

Figure 16b : Test 1A - Geotextile and HDPE Type 1, Shear Stress, τ (kN/m^2) Vs Strain (%)

In the case of geotextile and HDPE type 2 interface peak shear stresses were reached within strain of 4 to 5%. Continuous reduction in shear stresses were observed beyond peak , in the residual region unlike in the case of HDPE type 1. In all normal stresses there were pre peaks or slippage and minor plowing taking place before peak stresses. These indicate the shearing off HDPE texture with strain, losing the initial gripping forces between geotextile and HDPE Type 2. Internal failure of geotextile also took place, causing the geotextile ripped into two. Figure 16c shows the shear stress plots for interface test between geotextile and HDPE type 2 – Test 2A.

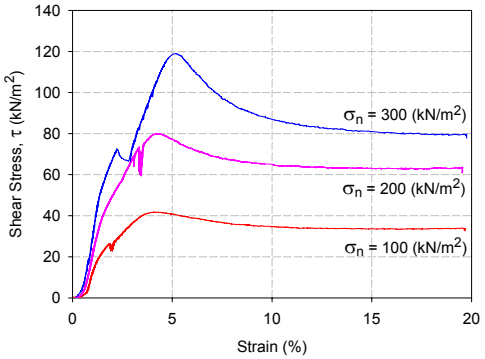

Figure 16c : Test 2A - Geotextile and HDPE Type 2, Shear Stress, τ (kN/m^2) Vs Strain (%)

Peak shear stresses were reached within strain of 4 to 6% for the case of geotextile and PVC (rear side) interface. The irregular trend of graphs was due to plowing effect during shearing. PVC was stretched about 5 to 25mm depending on normal stresses. Wavy formations were observed on PVC surfaces and internal failures of geotextile took place. These were due to cohesive forces between geotextile and PVC (rear side). Continuous increment in shear stresses was observed beyond 8% strain in the residual region. In all normal stresses there were pre peaks or slippage and minor plowing taking place before peak stresses. These indicate the loss of initial cohesive forces between geotextile and PVC (rear side). Figure 16d shows the shear stress plots for interface test between geotextile and PVC (rear side) – Test 3A.

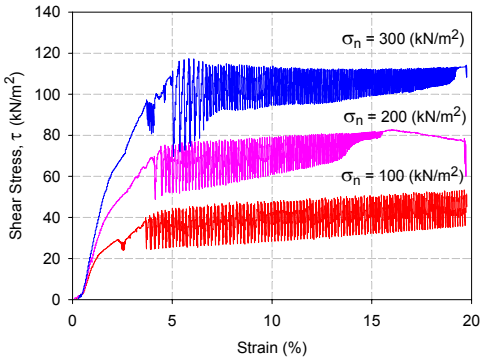

Figure 16d : Test 3A - Geotextile and PVC (rear side), Shear Stress, τ (kN/m^2) Vs Strain (%)

Peak shear stresses were reached within strain of 4 to 7% for the case of geotextile and PVC (front side) interface. The irregular trend of graphs was due to plowing effect during shearing. However unlike in the case of 3A, plowing effects were not observed in the residual region for high normal loads. PVC was stretched about 5 to 30mm depending on normal stresses. Wavy formations were observed on PVC surfaces and only partial internal failures of geotextile took place. Continuous increment in shear stresses was observed beyond 8% strain in the residual region for low normal stress.. In the case of higher normal stresses (200 and 300 kPa) reduction in residual shear stresses were observed in the residual region. In all normal stresses there were pre peaks or slippage and minor plowing taking place before peak stresses. These indicate the loss of initial cohesive of frictional forces between geotextile and PVC (front side). Figure 16e shows the shear stress plots for interface test between geotextile and PVC (front side) – Test 3C.

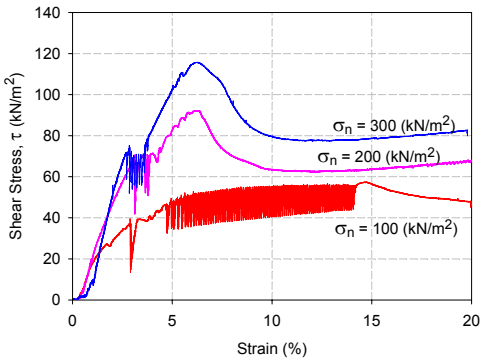

Figure 16e : Test 3C - Geotextile and PVC (front side), Shear Stress, τ (kN/m^2) Vs Strain (%)

In the case of geotextile and GCL Type 1 (Bentonite side) interface peak shear stresses were reached within strain of 4 to 6%. Shear stresses consistently reduce with strain beyond peak stresses. This could be due sliding within geotextile layer after internal failure of geotextile. Minor plowing force was observed between geotextile and GCL type 1 before peak forces were reached. In all normal stresses there were pre peaks or slippage and minor plowing taking place before peak stresses. These indicate the internal failure of geotextile and bentonite adhesive failure taking place. Figure 16f shows the shear stress plots for interface test between geotextile and GCL Type 1 (Bentonite side) – Test 4A.

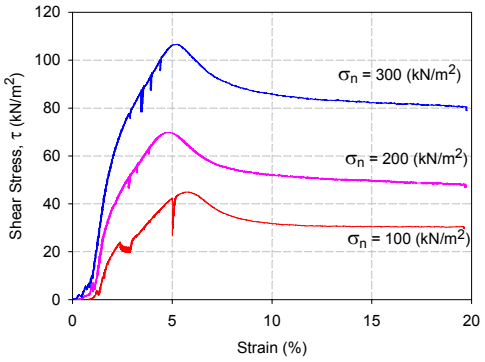

Figure 16f : Test 4A - Geotextile and GCL Type 1 (Bentonite side), Shear Stress, τ (kN/m^2) Vs Strain (%)

Peak shear stresses were reached within strain of 4 to 6%. Shear stresses consistently reduce with strain beyond peak stresses. This could be due to sliding between geotextile and HDPE of GCL. Plowing force was observed between geotextile and HDPE of GCL before peak forces were reached. In all normal stresses there were pre peaks or slippage and minor plowing taking place before peak stresses. Geotextiles were not ripped apart in these tests, however internal failures do took place. Figure 16g shows the shear stress plots for interface test between geotextile and GCL Type 1 (HDPE side) – Test 4C.

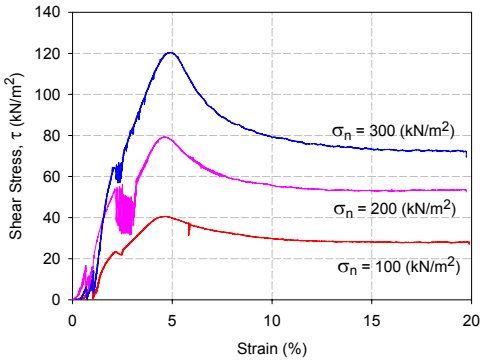

Figure 16g : Test 4C - Geotextile and GCL Type 1 (HDPE side), Shear Stress, τ (kN/m^2) Vs Strain (%)

Peak shear stresses were reached within strain of 4 to 5%. Shear stresses consistently reduce with strain beyond peak stresses and maintained constant residual shear stresses. Minor plowing force was observed between geotextile and woven geotextile of GCL Type 2 before peak forces were reached. In all normal stresses there were pre peaks or slippage and minor plowing taking place before peak stresses. Both geotextiles were not ripped apart in these tests. Figure 16h shows the shear stress plots for interface test between geotextile and GCL Type 2 (Woven side) – Test 5A.

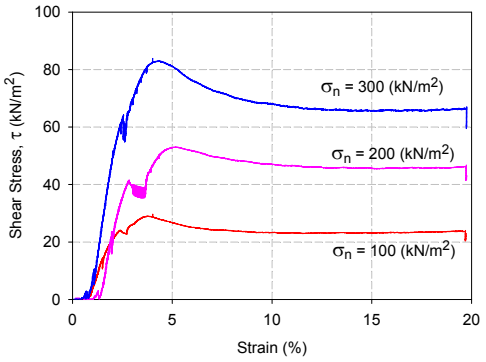

Figure 16h Test 5AC - Geotextile and GCL Type 2 (Woven side), Shear Stress, τ (kN/m^2) Vs Strain (%).

In the case of geotextile and GCL Type 2 (Non woven geotextile side) interface peak shear stresses were reached within strain of 4 to 5%. Shear stresses consistently reduce with strain beyond peak stresses and maintained constant residual shear stresses. Minor plowing force was observed between geotextile and non woven geotextile of GCL Type 2 before peak forces were reached. In all normal stresses there were pre peaks or slippage and minor plowing taking place before peak stresses. Residual shear stresses remain constant beyong 12% strain. Both geotextiles were not ripped apart in these tests. Figure 16i shows the shear stress plots for interface test between geotextile and GCL Type 2 (Non woven side) – Test 5C.

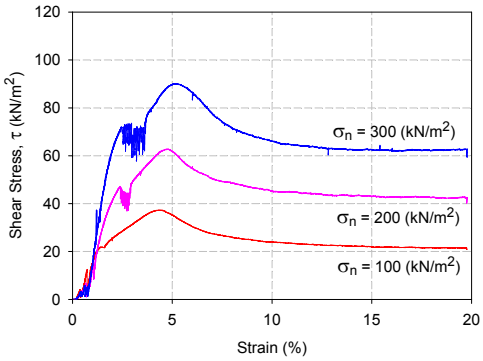

Figure 16i : Test 5C - Geotextile and GCL Type 2 (Non woven side), Shear Stress, τ (kN/m^2) Vs Strain (%)

To conclude the performance of geotextile with geomembrane and GCLs, in all cases expect HDPE type 1, plowing or slippage occurred before peak stresses. In some cases the geotextiles were ripped apart with internal failures.

5.2 HDPE Type 1 and 2 interfacing with GCLs

The performances of HDPEs were clearly distinguished between the case of smooth and textured surface. The fictional contribution of smooth surface HDPE was 7 to 9 degree. The textured surface of HDPE contributes frictional resistance in the range of 19 to 26 degree with increment of 10 to 15 in friction angle as compared to smooth surface HDPE. Details of the test results are presented in Table 6 and Figure 17a to 17i respectively. The results in Figure 17 also isolate HDPE type 1 which has low interface properties.

Table 6 : Test results of HDPE Type 1 and 2 interfacing with GCLs

Test	Interface Parameters	Cohesion (kN/m^2)	Friction Angle (^{O})
Interface Parameters Between HDPEs and PVC, GCLs			
TEST 6A	HDPE Type 1 & GCL Type 1 (Bentonite Side)	0.0	9.1
TEST 6C	HDPE Type 1 & GCL Type 1 (HDPE Side)	2.2	8.9
TEST 7A	HDPE Type 1 & GCL Type 2 (Non Woven Side)	2.2	7.8
TEST 7C	HDPE Type 1 & GCL Type 2 (Woven Side)	2.4	9.3
TEST 8A	HDPE Type 2 & GCL Type 1 (Bentonite Side)	28.8	19
TEST 8C	HDPE Type 2 & GCL Type 1 (HDPE Side)	0.0	19.9
TEST 9A	HDPE Type 2 & GCL Type 2 (Non Woven Side)	10.2	25.7
TEST 9C	HDPE Type 2 & GCL Type 2 (Woven Side)	2.1	23.2

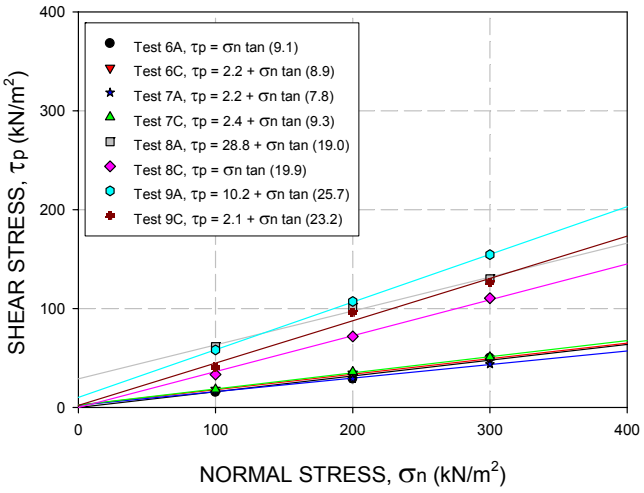

Figure 17a : Summary of peak failure envelopes for HDPE Type 1 and 2 interfacing with GCLs.

In the case of interface between HDPE type 1 and GCL type 1 (Bentonite side), the peak shear stresses were reached within strain of 2 to 2.5%. Shear stresses were maintained constantly in the residual region. No plowing kind of forces was observed, only minor slippage during shearing before peak stresses. The GCL bentonite was intact, no bentonite adhesive failure took place. Figure 17b shows the shear stress plots for interface test between HDPE type 1 and GCL type 1 (Bentonite side) – Test 6A

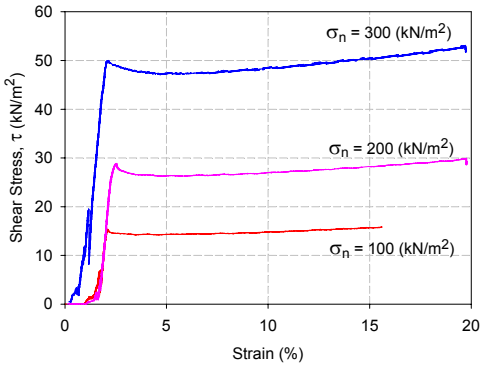

Figure 17b : Test 6A – HDPE Type 1 and GCL Type 1 (Bentonite side), Shear Stress, τ (kN/m^2) Vs Strain (%)

Peak shear stresses were reached within strain of 1 to 2.5%. Shear stresses beyond peak were maintained constant with minor increment in the residual region. No plowing force was observed between HDPE Type 1 and GCL Type 1 (HDPE side) before peak forces were reached. Both HDPE surface were in good condition. Figure 17c shows the shear stress plots for interface test between HDPE Type 1 and GCL Type 1 (HDPE side) – Test 6C.

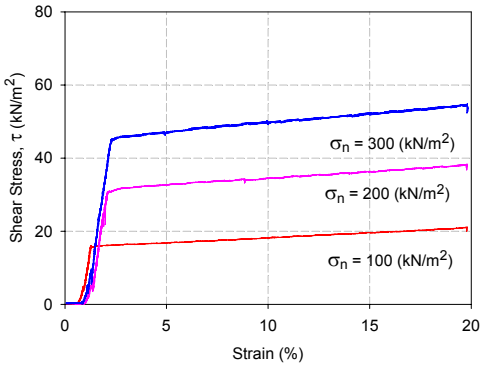

Figure 17c : Test 6C – HDPE Type 1 and GCL Type 1 (HDPE side), Shear Stress, τ (kN/m^2) Vs Strain (%)

For HDPE type 1 and GCL type 2 (non woven side) interface, the peak shear stresses were reached within strain of 1.5 to 2.5 %. Beyond peak stresses constant reduction in shear stresses were observed before minor increment in shear stresses in residual region. Continuous increment in shear stresses was observed beyond 10% strain in the residual region. The rate of residual shear stresses increment was relatively consistent for all normal stresses. Figure 17d shows the shear stress plots for interface test between HDPE type 1 and GCL type 2 (non woven side) – Test 7A.

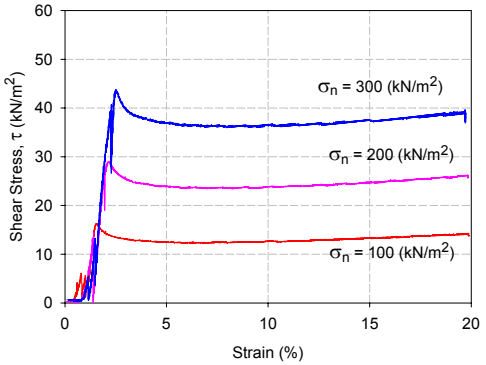

Figure 17d : Test 7A – HDPE Type 1 and GCL Type 2 (non woven side), Shear Stress, τ (kN/m^2) Vs Strain (%)

Peak shear stresses were reached within strain of 1 to 2 %. Shear stresses beyond peak were maintained constant in the residual region. No plowing force was observed between HDPE Type 1 and GCL Type 2 (woven side) before peak forces were reached. Both HDPE and woven geotextile surface were in good condition. Minor plowing or slippage occurred before peak shear stresses. Figure 17e shows the shear stress plots for interface test between HDPE Type 1 and GCL Type 2 (woven side) – Test 7C

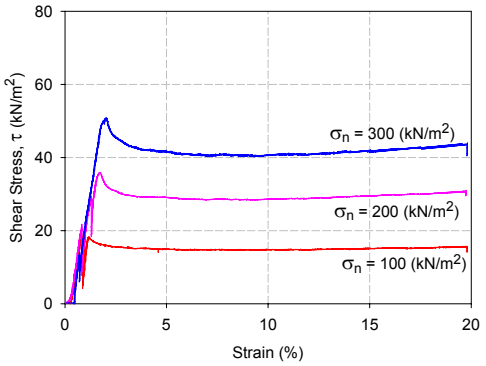

Figure 17e : Test 7C – HDPE Type 1 and GCL Type 2 (woven side), Shear Stress, τ (kN/m^2) Vs Strain (%)

For HDPE type 2 and GCL type 1 (bentonite side) interface, the peak shear stresses were reached within strain of 3 to 5 %. Beyond peak stresses constant reduction in shear stresses were observed before minor increment in shear stresses in residual region. In the case of lower normal stresses (100 kPa), the residual shear stress was maintain constant. The rate of residual shear stresses

increment was relatively consistent for 200 and 300 kPa normal stresses. In all normal stresses there were pre peaks or slippage and minor plowing taking place before peak stresses. These indicate the failure of bentonite adhesive failure taking place. Minor ripping of bentonite was observed for 100 kPa normal stress and total ripped off of bentonite was observed for 300 kPa normal stress. Figure 17f shows the shear stress plots for interface test between HDPE type 2 and GCL type 1 (bentonite side) – Test 8A.

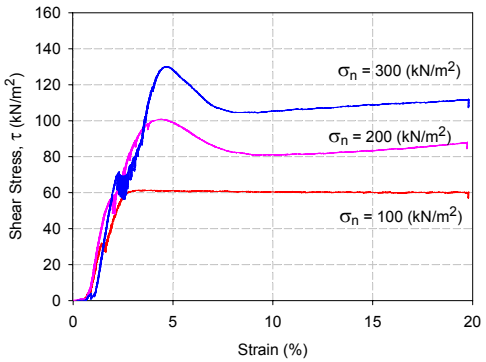

Figure 17f : Test 8A – HDPE Type 2 and GCL Type 1 (bentonite side), Shear Stress, τ (kN/m^2) Vs Strain (%)

Peak shear stresses were reached within strain of 4 to 5 %. Shear stresses beyond peak, consistently reduced before remaining constant in the residual region. No plowing force was observed between HDPE Type 2 and GCL Type 1 (HDPE side) before peak forces was reached. HDPE type 2 textured surfaces were shear between 20 to 70% depending on the normal stresses. Minor smoothening took place on GCL type 1 (HDPE side). GCL type 1 (HDPE side) texture is much harder than HDPE type 2 texture. Figure 17g shows the shear stress plots for interface test between HDPE Type 2 and GCL Type 1 (HDPE side) – Test 8C

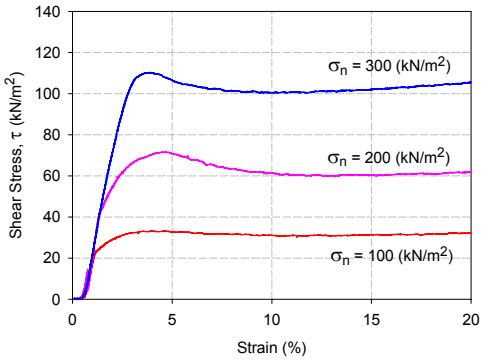

Figure 17g : Test 8C – HDPE Type 2 and GCL Type 1 (HDPE side), Shear Stress, τ (kN/m^2) Vs Strain (%)

For HDPE type 2 and GCL type 2 (non woven side) interface, the peak shear stresses were reached within strain of 4 to 6 %. Beyond peak stresses constant reduction in shear stresses were observed and maintained constant in the residual region. In the case of lower normal stresses (100 and 200 kPa), the residual shear stresses were maintain constant. As for the 300 kPa normal stress the wavy formation in residual region was due to tension failure of geotextiles. Both non woven and woven geotextile of GCls were torn. The surface of textured HDPE was not damaged. In all normal stresses there were pre peaks or slippage and minor plowing taking place before peak stresses. Figure 17h shows the shear stress plots for interface test between HDPE type 2 and GCL type 2 (non woven side) – Test 9A.

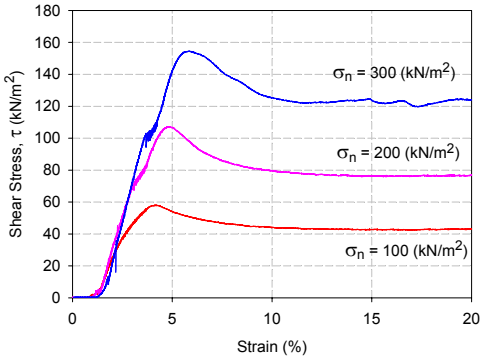

Figure 17h : Test 9A – HDPE Type 2 and GCL Type 2 (non woven side), Shear Stress, τ (kN/m^2) Vs Strain (%)

In the case of HDPE type 2 and GCL type 2 (woven side) interfaces, the peak shear stresses were reached within strain of 3 to 5 %. Beyond peak stresses constant reduction in shear stresses were observed and maintained constant in the residual region. In the case of lower normal stresses (100 and 200 kPa), the residual shear stresses were maintain constant. As for the 300 kPa normal stress the wavy formation in residual region was due to tension failure of geotextiles. Only woven geotextile of GCl was torn. The surface of textured HDPEs was sheared from partially to fully sheared surface. In all normal stresses there were no pre peaks, slippage or plowing taking place before peak stresses. Figure 17i shows the shear stress plots for interface test between HDPE type 2 and GCL type 2 (woven side) – Test 9C.

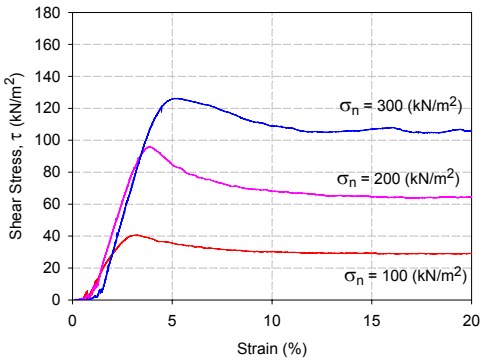

Figure 17i : Test 9C – HDPE Type 2 and GCL Type 2 (woven side), Shear Stress, τ (kN/m^2) Vs Strain (%)

The residual shear stresses were lower as compared to peak shear stresses in the case of HDPE type 2. As for HDPE type 2 residual shear stresses are higher then peak shear stresses. Increment in shear stresses was observed in the residual region for HDPE type 1. HDPE type 1 exhibits low interface parameters however able to sustain constant shear stresses with strain in the residual region. Higher residual shear stresses are crucial when strain incompatibility assessment is made out of liner component members.

5.3 PVC interfacing with GCLs

The performances of PVC with GCLs had wide range of interface test results. The fictional contribution of PVC is between 15 to 26 degree, while cohesions were in the range of 0 to 24 kN/m^2. The performance of PVC (front side) had higher frictional resistance with GCL type 1 as compared to PVC (rear side). The same applies for PVC (front side) with GCL type 2, however the different are marginal. Details of the test results are presented in Table 7 and Figure 18a to 18f respectively.

Table 9 : Test results of PVC interfacing with GCLs

Test	Interface Parameters	Cohesion (kN/m^2)	Friction Angle (^{o})
Interface Parameters Between PVC and GCLs			
TEST 10A	PVC (Rear Side) & GCL Type 1 (Bentonite Side)	17.6	18.1
TEST 10C	PVC (Rear Side) & GCL Type 1 (HDPE Side)	12.1	20.0
TEST 10E	PVC Front Side & GCL Type 1 (Bentonite Side)	0.0	26.3
TEST 10G	PVC (Front Side) & GCL Type 1 (HDPE Side)	0.0	25.2
TEST 11A	PVC (Rear Side) & GCL Type 2 (Non Woven Side)	17.2	15.3
TEST 11C	PVC (Rear Side) & GCL Type 2 (Woven Side)	14.7	18.1
TEST 11E	PVC Front Side & GCL Type 2 (Non Woven Side)	10.0	17.4
TEST 11G	PVC (Front Side) & GCL Type 2 (Woven Side)	24.0	18.4

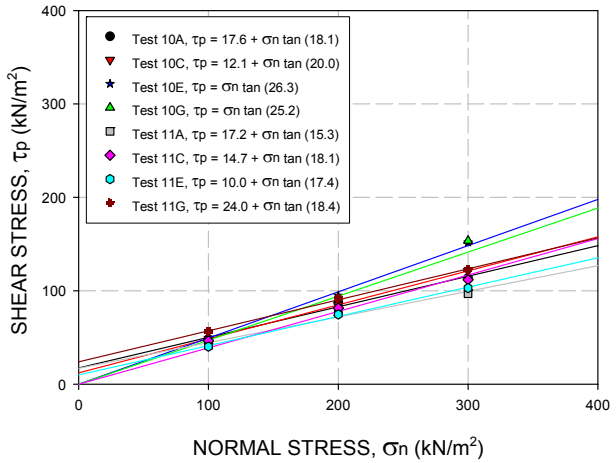

Figure 18a : Summary of peak failure envelopes for PVC interfacing with GCLs

For PVC (rear side) and GCL type 1 (bentonite side) interface, the peak shear stresses were reached within strain of 2 to 4 %. Adhesive failure of bentonite took place however it was not total failure. Continuous increment in shear stresses was observed beyond 6 % strain. The increment could be due to strong cohesive forces between PVC (rear side) and GCL type 1 (bentonite side). The sudden drop in shear stresses for normal loads of 200 and 300 kPa was due to adhesive failure of bentonite. In all normal stresses there were pre peaks or slippage before peak stresses. Figure 18b shows the shear stress plots for interface test between PVC (rear side) and GCL type 1 (bentonite side) – Test 10A

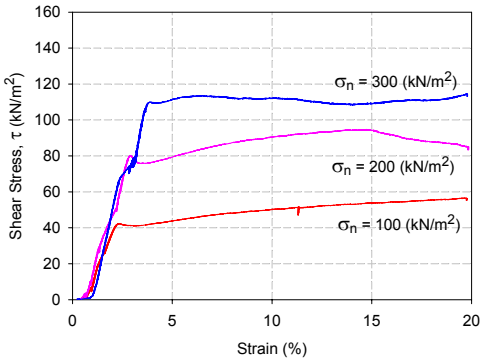

Figure 18b : Test 10A – PVC (rear side) and GCL Type 1 (bentonite side), Shear Stress, τ (kN/m2) Vs Strain (%)

In the case of PVC (rear side) and GCL type 1 (HDPE side) interface peak shear stresses were reached within strain of 1 to 2.5 %. The surface of both PVC and HDPE were in good condition.

Continuous increments in shear stresses were observed in the residual region beyond 5% strain. Pre peaks were observed for normal loads of 100 and 200 kPa. Figure 18c shows the shear stress plots for interface test between PVC (rear side) and GCL type 1 (bentonite side) – Test 10C

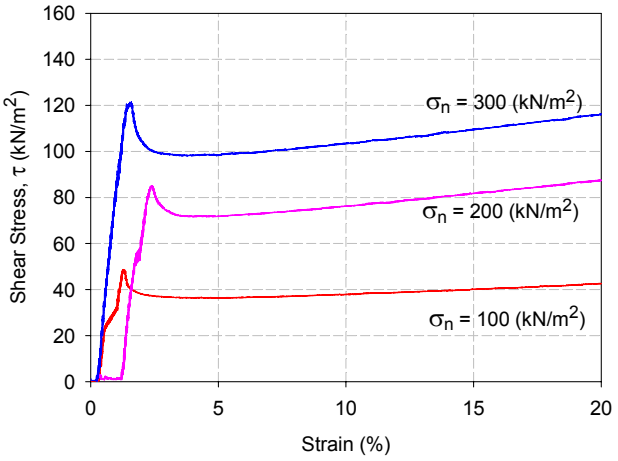

Figure 18c : Test 10C – PVC (rear side) and GCL Type 1 (HDPE side), Shear Stress, τ (kN/m^2) Vs Strain (%)

For PVC (front side) and GCL type 1 (bentonite side) the peak shear stresses were reached within strain of 3 to 4%. Adhesive failure of bentonite took place for normal loads of 200 kPa and 300 kPa. In general continuous increments in shear stresses were observed in the residual region. Minor slippages were observed before peak stresses were reached. Figure 18d shows the shear stress plots for interface test between PVC (front side) and GCL type 1 (bentonite side) – Test 10E

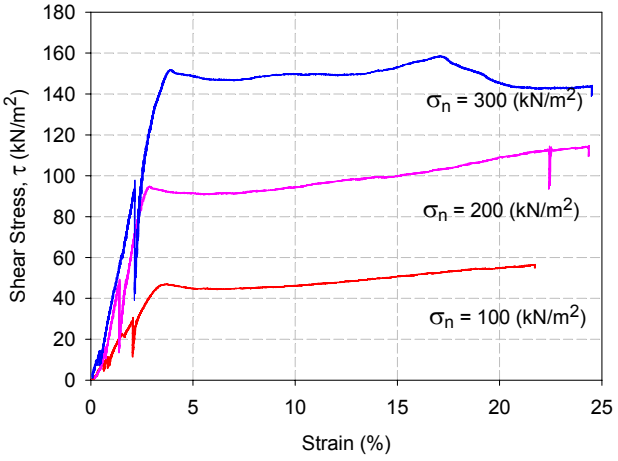

Figure 18d : Test 10E – PVC (front side) and GCL Type 1 (bentonite side), Shear Stress, τ (kN/m^2) Vs Strain (%)

As for PVC (front side) and GCL type 1 (HDPE side), peak shear stresses were reached within strain of 1 to 3%. Continuous increments in shear stresses were observed beyond 8% strain. The rate of shear stress increment in the residual region is reasonable consistence for all normal loads. Minor slippage and pre peaks were observed for all normal loads. Figure 18e shows the shear stress plots for interface test between PVC (front side) and GCL type 1 (HDPE side) – Test 10G

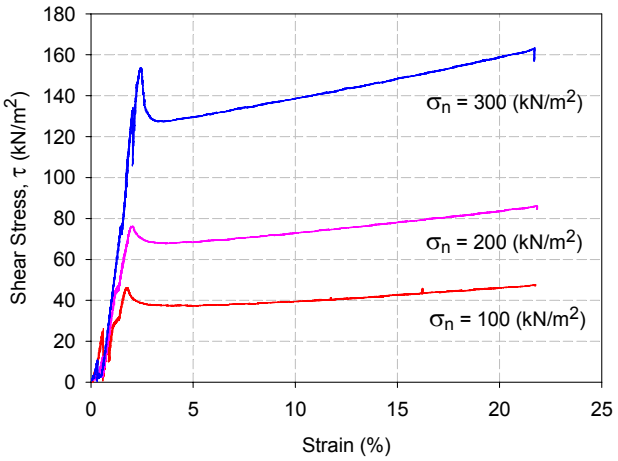

Figure 18e : Test 10G – PVC (front side) and GCL Type 1 (HDPE side), Shear Stress, τ (kN/m^2) Vs Strain (%)

In the case of PVC (rear side) and GCL type 2 (non woven side) interfaces, the peak shear stresses were reached within strain of 4 to 6 %. Beyond peak stresses the residual shear stresses were maintain constant. The geotextiles were not torn during the test. In all normal stresses there were pre peaks or slippage and minor plowing taking place before peak stresses. Figure 18f shows the shear stress plots for interface test between PVC (rear side) and GCL type 2 (non woven side) – Test 11A.

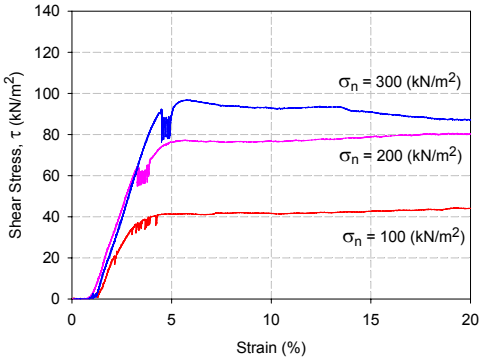

Figure 18f : Test 11A – PVC (rear side) and GCL Type 2 (non woven side), Shear Stress, τ (kN/m^2) Vs Strain (%)

For PVC (rear side) and GCL type 2 (woven side) interface, the peak shear stresses were reached within strain of 3 to 6 %. Continuous increment in shear stresses was observed for normal load of 100 kPa. Residual shear stress trend various for higher normal loads of 200 and 300 kPa. The increment in shear stresses in the residual region was due to high cohesion forces. In all normal stresses there were no pre peaks, slippage or plowing taking place before peak stresses. Figure 18g shows the shear stress plots for interface test between PVC (rear side) and GCL type 2 (woven side) – Test 11C

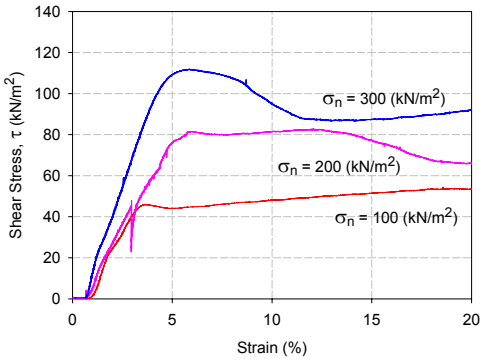

Figure 18g : Test 11C – PVC (rear side) and GCL Type 2 (woven side), Shear Stress, τ (kN/m^2) Vs Strain (%)

In the case of PVC (front side) and GCL type 2 (non woven side) interfaces, the peak shear stresses were reached within strain of 4 to 8 %. Beyond peak stresses constant reduction in shear stresses were observed and maintained constant in the residual region. In all normal stresses there were no pre peaks, slippage or plowing taking place before peak stresses. Figure 18h shows the shear stress plots for interface test between PVC (front side) and GCL type 2 (non woven side) – Test 11E.

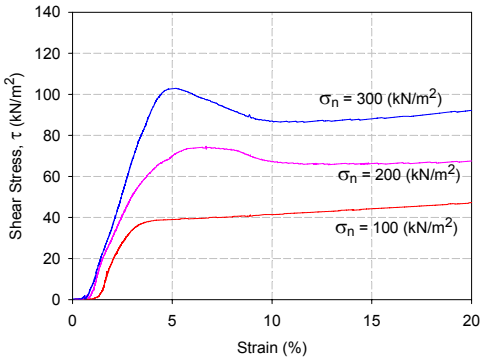

Figure 18h : Test 11E – PVC (front side) and GCL Type 2 (non woven side), Shear Stress, τ (kN/m^2) Vs Strain (%)

For PVC (front side) and GCL type 2 (woven side) interfaces, the peak shear stresses were reached within strain of 4 to 8 %. Beyond peak stresses constant reduction in shear stresses were observed and maintained constant in the residual region. The high and constant residual shear stresses could be due to cohesion contribution of bentonite in the GCL. In all normal stresses there were pre peaks taking place before peak stresses. Figure 18i shows the shear stress plots for interface test between PVC (front side) and GCL type 2 (woven side) – Test 11G.

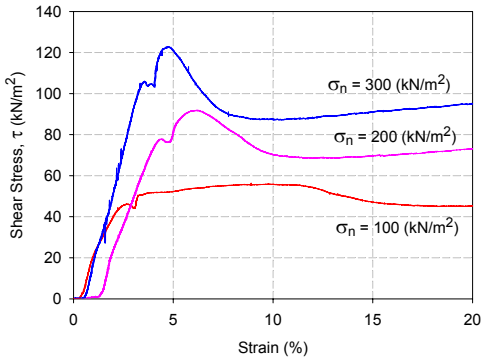

Figure 18i : Test 11G – PVC (front side) and GCL Type 2 (woven side), Shear Stress, τ (kN/m^2) Vs Strain (%)

The trend of failure mode for both sides of PVC in gerenal was consistent. The shear stresses in residual regions are lower for all the cases except for interface with HDPE side of GCL type 1 and woven side of GCL type 2.

5.4 Silt bentonite (100 : 10) interfacing with geosynthetics

The performances of silt bentonite mixture (100 : 10) with geosynthetics were relatively consistent with interface test results were within narrow range of differences. Only fictional contribution was exhibited without cohesions. The performance of geotextile and HDPE type 1 was the lowest with fiction angle of 15 degrees. HDPE type 2 and PVC provide high and relatively similar frictional resistance. Details of the test results are presented in Table 8 and Figure 19a to 19f respectively.

Table 8 : Test results of silt bentonite (100 : 10) interfacing with geosynthetics

Test	Interface Parameters	Cohesion (kN/m^2)	Friction Angle (^{0})
Interface Parameters Between Geosynthetic and Silt Bentonite Mixture (100 : 10) CCL			
TEST 12A	GEOTEXTILE & SILT BENTONITE Mix(100 : 10)	0.0	15.3
TEST 13A	HDPE Type 1 & SILT BENTONITE Mix (100 : 10)	0.0	15.4
TEST 14A	HDPE Type 2 & SILT BENTONITE Mix (100 : 10)	0.0	24.2
TEST 15A	PVC (Rear Side) & SILT BENTONITE Mix (100 : 10)	0.0	22.2
TEST 15C	PVC (Front Side) & SILT BENTONITE Mix (100 : 10)	0.0	20.0

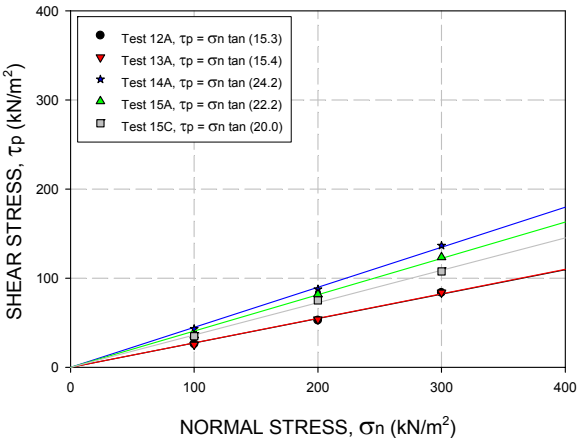

Figure 19a : Summary of peak failure envelopes for Silt bentonite (100 : 10) interfacing with Geosnthetics

For silt bentonite (100 : 10) and geotextile interface, the peak shear stresses were reached within strain of 5 to 6.5 %. There were spots of tearing and total internal failure of geotextile took place. Continuous reduction in the shear stresses was observed until constant residual shear stresses were obtained beyong 10% strain. In all normal stresses there were no pre peaks, slippage or plowing taking place before peak stresses. Figure 19b shows the shear stress plots for interface test between silt bentonite (100 : 10) and geotextile – Test 12A

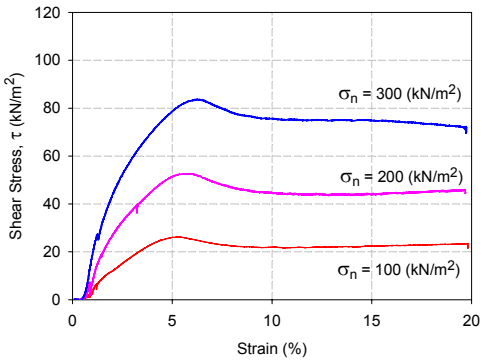

Figure 19b : Test 12A – Silt bentonite (100 : 10) and Geotextile, Shear Stress, τ (kN/m^2) Vs Strain (%)

In the case of interface between silt bentonite (100 : 10) and HDPE type 1, the peak shear stresses were reached within strain of 2 to 3%. Continuous reduction of shear stresses was observed beyond peak stresses before constant or minor increment in shear stresses was observed 10% strain onwards. No plowing kind of forces was observed, only in case with the normal load of 300 kPa minor plowing was observed beyond peak stresses. Figure 19c shows the shear stress plots for interface test between silt bentonite (100 : 10) and HDPE type 1 – Test 13A

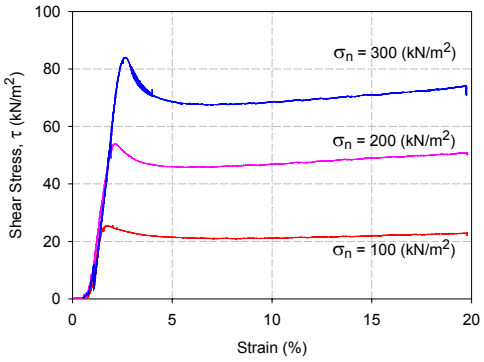

Figure 19c : Test 13A – Silt bentonite (100 : 10) and HDPE type 1, Shear Stress, τ (kN/m^2) Vs Strain (%)

For silt bentonite (100 : 10) and HDPE type 2 interface, the peak shear stresses were reached within strain of 5 to 8 %. The texture of HDPE type 2 was not sheared. Continuous increment in shear stresses was observed for normal loads of 100 and 200 kPa in the residual region. In all normal stresses there were pre peaks or slippage and minor plowing taking place before peak stresses. Figure 19d shows the shear stress plots for interface test between silt bentonite (100 : 10) and HDPE type 2 – Test 14A

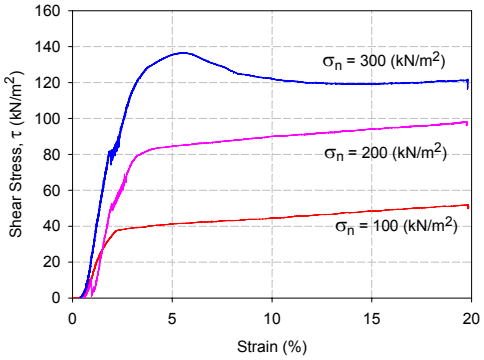

Figure 19d : Test 14A – Silt bentonite (100 : 10) and HDPE type 2, Shear Stress, τ (kN/m^2) Vs Strain (%)

In the case of interface between silt bentonite (100 : 10) and PVC (rear side), the peak shear stresses were reached within strain of 5 to 8%. Continuous reduction of shear stresses was observed beyond peak stresses for normal loads of 200 and 300 kPa. However constant residual stresses were maintained for normal load of 100 kPa. No plowing kind of forces was observed, in the test. Pre peak stresses were clearly observed for normal load of 300 kPa only. Figure 19e shows the shear stress plots for interface test between silt bentonite (100 : 10) and PVC (rear side) – Test 15A

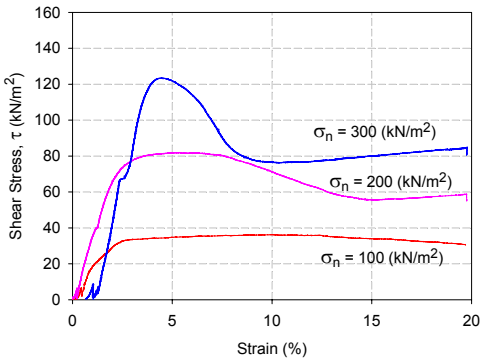

Figure 19e : Test 15A – Silt bentonite (100 : 10) and PVC (rear side), Shear Stress, τ (kN/m^2) Vs Strain (%)

For silt bentonite (100 : 10) and PVC (front side) interface, the peak shear stresses were reached within strain of 4 to 8 %. Continuous reduction of shear stresses was observed beyond peak stresses for normal loads of 200 and 300 kPa. However constant residual stresses were maintained for normal load of 100 kPa. In all normal stresses there were pre peaks or slippage and minor plowing taking place before peak stresses. Figure 19f shows the shear stress plots for interface test between silt bentonite (100 : 10) and PVC (front side) – Test 15C

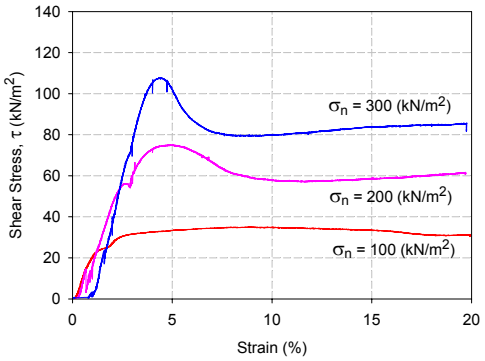

Figure 19f : Test 15C – Silt bentonite (100 : 10) and PVC (front side), Shear Stress, τ (kN/m^2) Vs Strain (%)

Eventhough HDPE Type 1 and geotextile had low frictional resistance, the interface values are higher as compared to direct interface between geotextile and HDPE Type 1. Hence it is proposed to sandwich HDPE Type 1 or geomembrane in general within compacted clay liner (CCL), shown in Figure 19g, rather than placing on top of geotextile, as shown in Figure 19h. Precautions are required to avoid damages on geomembrane during installation of compacted clay liner (CCL) due to direct contact. It is recommended to allow for some sacrificial thickness on geomembrane to resists major or microscopic puncture.

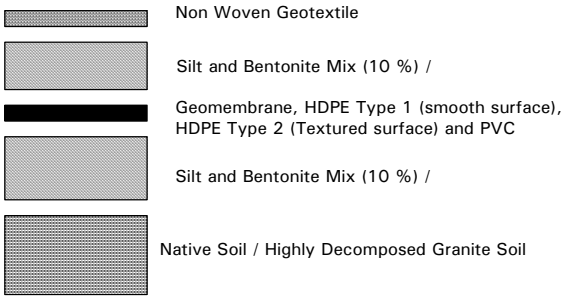

Figure 19g : Single composite liner configuration

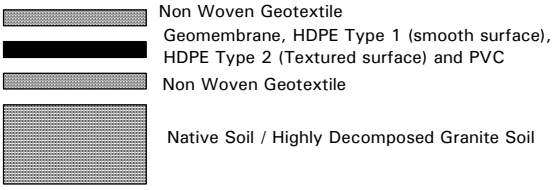

Figure 19h : Single membrane liner configuration

5.5 Silt bentonite (100 : 10) interfacing with GCLs Type 1 and 2

The performances of silt bentonite mixture (100 : 10) with geosynthetics clay liners (GCL) were relatively consistent with interface test results within a narrow range of differences. Higher cohesion and lower frictional contribution was observed with GCL type 1 (bentonite side). Higher fiction was observed in the case of GCL type 1 (HDPE side) and GCL type 2 (woven side). In general both GCLs sides contributed high frictional resistance with silt bentonite (100 : 10). Details of the test results are presented in Table 9 and Figure 20a to 20e respectively.

Table 9 : Test results of silt bentonite (100 : 10) interfacing with geosynthetics

Test	Interface Parameters	Cohesion (kN/m^2)	Friction Angle (^{o})
Interface Parameters Between GCLs and Silt Bentonite Mixture (100 : 10) CCL			
TEST 17A	GCL Type 1 (Bentonite Side) & SILT BENTONITE Mix (100 : 10)	13.9	17.0
TEST 17C	GCL Type 1 (HDPE Side) & SILT BENTONITE Mix (100 : 10)	0.0	22.6
TEST 18A	GCL Type 2 (Non Woven Side) & SILT BENTONITE Mix (100 : 10)	6.2	20.8
TEST 18C	GCL Type 2 (Woven Side) & SILT BENTONITE Mix (100 : 10)	1.4	21.4

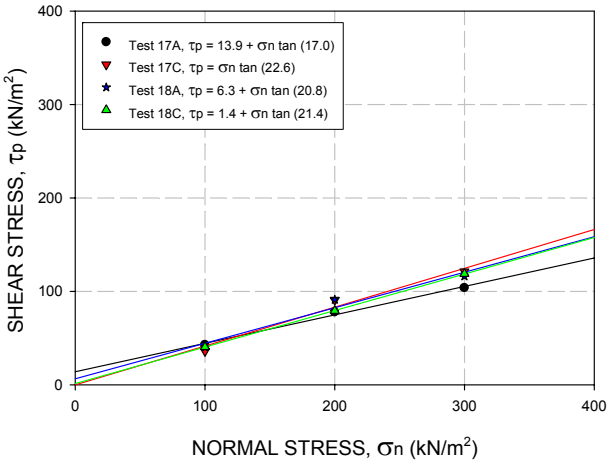

Figure 20a : Summary of peak failure envelopes for Silt bentonite (100 : 10) interfacing with GCLs

For silt bentonite (100 : 10) and GCL type 1 (bentonite side) interface, the peak shear stresses were reached within strain of 5 to 6.5 %. Beyond peak the shear stresses were maintained constant in the residual region. The surface of bentonite was pressed and smoothed by the normal loads. In all normal stresses there were no pre peaks or slippage or plowing taking place before peak stresses. Figure 22b shows the shear stress plots for interface test between silt bentonite (100 : 10) and GCL type 1 (bentonite side) – Test 17A

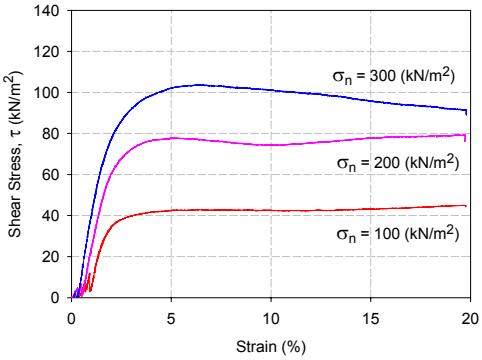

Figure 20b : Test 17A – Silt bentonite (100 : 10) and GCL type 1 (bentonite side), Shear Stress, τ (kN/m^2) Vs Strain (%)

In the case of interface between silt bentonite (100 : 10) and GCL type 1 (HDPE side), the peak shear stresses were reached within strain of 6 to 8%. Due to GCL elongation, plastic deformation occurred at clamp area. However texture of HDPE remains intact. Beyond peak the shear stresses were maintained constant in the residual region for normal loads of 100 and 200 kPa . For 300 kPa normal loads reduction in shear stresses beyond peak was observed before constant residual shear stresses reached. No plowing kind of forces was observed, in the test. Only minor slippage occurred. Figure 20c shows the shear stress plots for interface test between silt bentonite (100 : 10) and GCL type 1 (HDPE side) – Test 17C

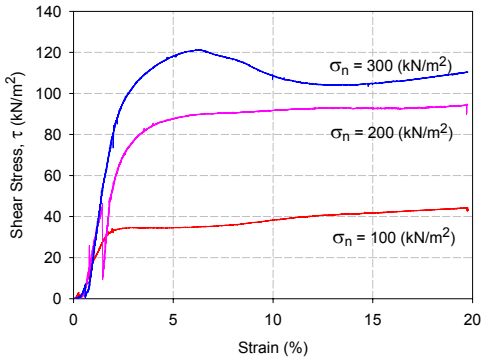

Figure 20c : Test 17C – Silt bentonite (100 : 10) and GCL type 1 (HDPE side), Shear Stress, τ (kN/m^2) Vs Strain (%)

Silt bentonite (100 : 10) and GCL type 2 (non woven side) interface, the peak shear stresses were reached within strain of 6 to 8 %. Beyond peak stresses constant residual shear stresses were obtained for all normal loads. Fluctuation in shear stresses in the residual region for normal loads of 200 and 300 kPa were due to tearing of geotextile during the test. In all normal stresses there were no peaks or slippage or plowing taking place before peak stresses. Figure 20c shows the shear stress plots for interface test between silt bentonite (100 : 10) and GCL type 2 (non woven side) – Test 18A

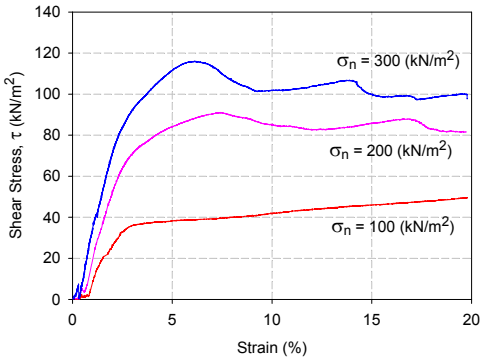

Figure 20d : Test 18A – Silt bentonite (100 : 10) and GCL type 2 (non woven side), Shear Stress, τ (kN/m^2) Vs Strain (%)

In the case of interface between silt bentonite (100 : 10) and GCL type 2 (woven side), the peak shear stresses were reached within strain of 6 to 8%. Beyond peak stresses constant residual shear stresses were obtained for all normal loads. Fluctuation in shear stresses in the residual region for normal load of 300 kPa was due to tearing of geotextile during the test. In all normal stresses there were minor slippages or plowing taking place before peak stresses. Figure 20d shows the shear stress plots for interface test between silt bentonite (100 : 10) and GCL type 2 (woven side) – Test 18C

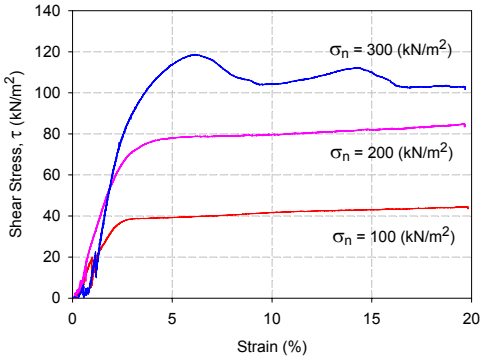

Figure 20e : Test 18C – Silt bentonite (100 : 10) and GCL type 2 (woven side), Shear Stress, τ (kN/m^2) Vs Strain (%)

GCL interface test results were very much similar of those from HDPE Type 2 and PVC interface with silt bentonite

5.6 Sand bentonite (100 : 10) interfacing with geosynthetics

The performances of sand bentonite mixture (100 : 10) with geosynthetics were covered in wide range of friction angle. Only fictional contribution was exhibited without cohesions. The performance of geotextile and HDPE type 1 were the lowest with fiction angle of 13 to 15 degrees. HDPE type 2 and PVC provide high and relatively similar frictional resistance. However friction angle of PVC front side was as low as geotextile friction angle. Details of the test results are presented in Table 10 and Figure 21a to 21f respectively.

Table 10 : Test results of sand bentonite (100 : 10) interfacing with geosynthetics

Test	Interface Parameters	Cohesion (kN/m^2)	Friction Angle (^{O})
Interface Parameters Between Geosynthetic and Sand Bentonite Mixture (100 : 10) CCL			
TEST 19A	GEOTEXTILE & SAND BENTONITE Mix (100 : 10)	0.0	15.8
TEST 20A	HDPE Type 1 & SAND BENTONITE Mix (100 : 10)	0.0	13.8
TEST 21A	HDPE Type 2 & SAND BENTONITE Mix (100 : 10)	0.0	24.5
TEST 22A	PVC (Rear Side) & SAND BENTONITE Mix (100 : 10)	0.0	19.8
TEST 22C	PVC (Front Side) & SAND BENTONITE Mix (100 : 10)	0.0	16.9

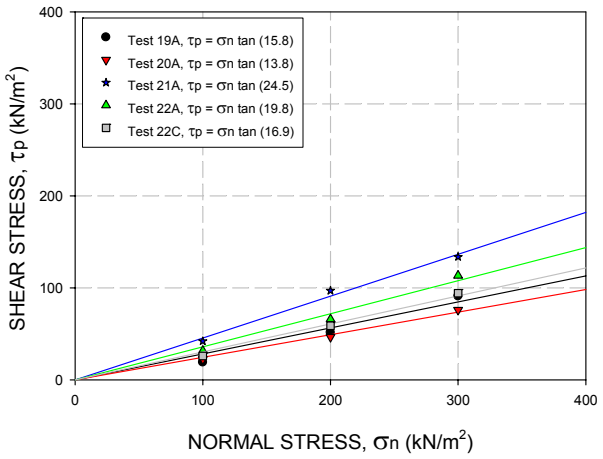

Figure 21a : Summary of peak failure envelopes for Silt bentonite (100 : 10) interfacing with geosynthetics

Sand bentonite (100 : 10) and geotextile interface, the peak shear stresses were reached within strain of 3 to 8 %. Continuous increment in shear stresses was observed beyond peak stresses into residual region. The geotextile was split into two during the tests. The residual shear stress behaviours were relatively similar for normal loads of 200 and 300 kPa.In all normal stresses there were no pre peaks or slippage or plowing taking place before peak stresses. Figure 21c shows the shear stress plots for interface test between silt bentonite (100 : 10) and geotextile – Test 19A

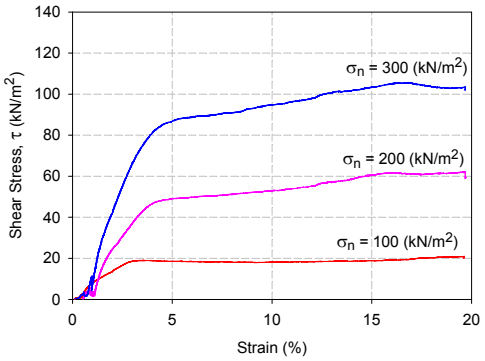

Figure 21b : Test 19A – Sand bentonite (100 : 10) and geotexttile, Shear Stress, τ (kN/m^2) Vs Strain (%)

In the case of interface between sand bentonite (100 : 10) and HDPE type 1, the peak shear stresses were reached within strain of 1 to 2.5 %. Minor reduction of shear stresses was observed beyond peak stresses before constant shear stresses were observed in the residual region. The trends of shear stresses were similar for all tests. No plowing kind of forces was observed, in the tests. Figure 21c shows the shear stress plots for interface test between sand bentonite (100 : 10) and HDPE type 1 – Test 20A

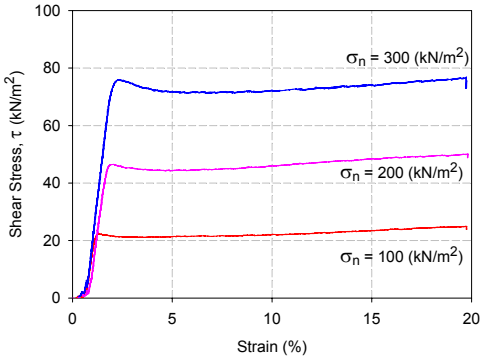

Figure 21c : Test 20A – Sand bentonite (100 : 10) and HDPE type 1, Shear Stress, τ (kN/m^2) Vs Strain (%)

For sand bentonite (100 : 10) and HDPE type 2 interface, the peak shear stresses were reached within strain of 7 to 8 %. The texture of HDPE type 2 was sheared partially to fully as the normal loads were increased. Constant increments in shear stresses were observed beyond peak stresses in the residual region. In all normal stresses there were pre peaks taking place before peak stresses. Figure 21d shows the shear stress plots for interface test between sand bentonite (100 : 10) and HDPE type 2 – Test 21A

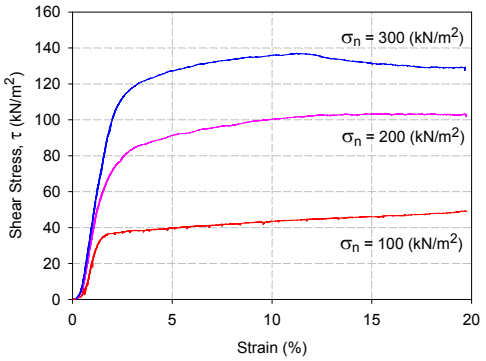

Figure 21d : Test 21A – Sand bentonite (100 : 10) and HDPE type 2, τ (kN/m^2) Vs Strain (%)

Sand bentonite (100 : 10) and PVC (rear side) interface, the peak shear stresses were reached within strain of 6 to 8 %. Continuous increment in shear stresses was observed beyond peak stresses till constant residual stresses were reached into residual region for normal loads of 100 and 200 kPa. The trend shear stresses for normal loads of 300 kPa were much different then lower normal loads. There were minor pre peaks for normal loads of 200 and 300 kPa. Figure 21e shows the shear stress plots for interface test between sand bentonite (100 : 10) and PVC (rear side) – Test 22A

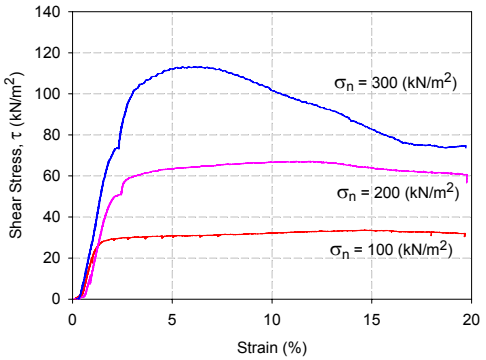

Figure 21e : Test 22A – Sand bentonite (100 : 10) and PVC (rear side), τ (kN/m^2) Vs Strain (%)

In the case of interface between sand bentonite (100 : 10) and PVC (front side), the peak shear stresses were reached within strain of 2 to 8 %. Constant shear stresses were observed beyond peak stresses in the residual region. However in the case of normal load of 300 kPa, gradual reduction in shear stresses was observed before constant shear stresses were reached in the residual region. No plowing kind of forces was observed, only minor slippages in the tests. Figure 21f shows the shear stress plots for interface test between sand bentonite (100 : 10) and PVC (front side) – Test 22C

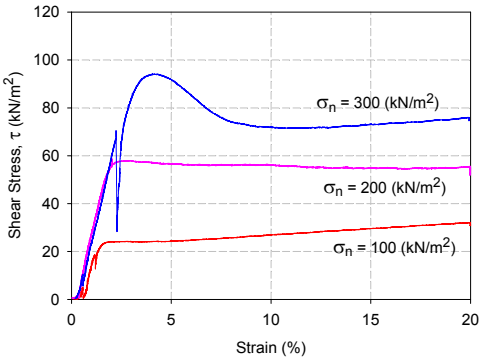

Figure 21f : Test 22C – Sand bentonite (100 : 10) and PVC (front side), τ (kN/m^2) Vs Strain (%)

The performance of silt bentonite mixture (100 : 10) and sand bentonite mixture (100 : 10) with geosynthetics were consistent. However the friction contribution of sand bentonite was marginally lower compared to silt bentonite mixture (100 : 10). Initial prediction, sand was believed to provide higher frictional resistance as compared to silt. However the test results were not as predicted due to the presents of bentonite in sand and higher damage were created on interfacing member during shearing by sand.

5.7 Sand bentonite (100 : 10) interfacing with GCLs Type 1 and 2

The performances of sand bentonite mixture (100 : 10) with GCL type 1 and 2 were covered with narrow minimum and maximum range. Cohesion was not contributed in the case of GCL type 2 (non woven side). GCL type 1 (HDPE side) has the lowest friction angle. GCL type 1 (bentonite side) and GCL type 2 (woven side) frictional resistance was 17 degree, however GCL type 2 (woven side) contributed high cohesion. Details of the test results are presented in Table 11 and Figure 22a to 22e respectively.

Table 11 : Test results of sand bentonite (100 : 10) interfacing with geosynthetics

Test	Interface Parameters	Cohesion (kN/m^2)	Friction Angle (^{O})
Interface Parameters Between GCLs and Sand Bentonite Mixture (100 : 10) CCL			
TEST 24A	GCL Type 1 (Bentonite Side) & SAND BENTONITE Mix (100 : 10)	6.5	17.6
TEST 24C	GCL Type 1 (HDPE Side) & SAND BENTONITE Mix (100 : 10)	14.7	13.7
TEST 25A	GCL Type 2 (Non Woven Side) & SAND BENTONITE Mix (100 : 10)	0.0	22.6
TEST 25C	GCL Type 2 (Woven Side) & SAND BENTONITE Mix (100 : 10)	25.8	17.1

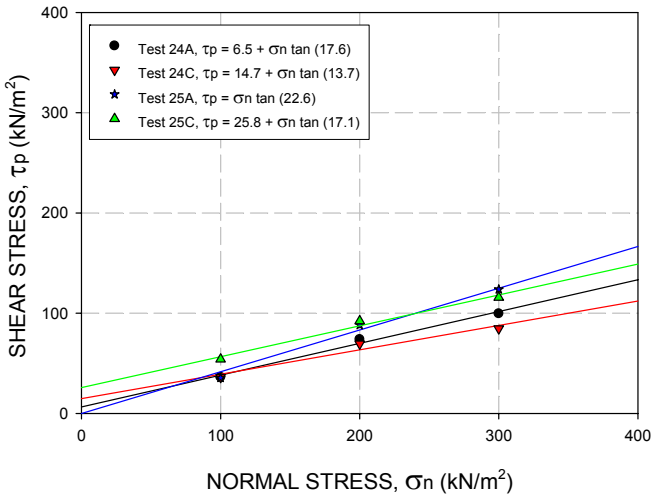

Figure 22a : Summary of peak failure envelopes for Sand bentonite (100 : 10) interfacing with GCLs Type 1 and 2

For sand bentonite (100 : 10) and GCL type (bentonite side) interface, the peak shear stresses were reached within strain of 3 to 4.5 %. GCL bentonite surface was partially to fully sheared base on normal load. Constant shear stresses were observed beyond peak stresses in the residual region. However in the case of normal load of 300 kPa, gradual reduction in shear stresses was observed before constant shear stresses were reached in the residual region. No plowing kind of forces was observed. Figure 22b shows the shear stress plots for interface test between sand bentonite (100 : 10) and GCL type 1 (bentonite side) – Test 24C

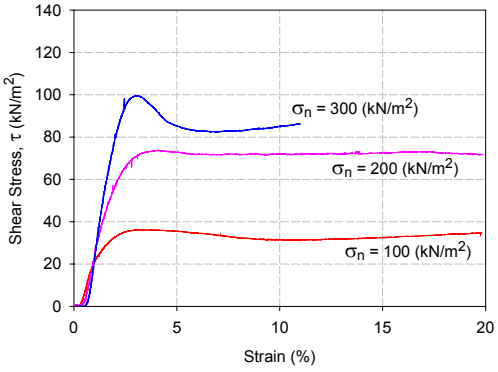

Figure 22b : Test 24A – Sand bentonite (100 : 10) and GCL type 1 (bentonite side), τ (kN/m^2) Vs Strain (%)

Sand bentonite (100 : 10) and GCL type 1 (HDPE side) interface, the peak shear stresses were reached within strain of 6 to 8 %. The surface of GCL HDPE was sheared smooth, and internal failure of bentonite took place. Continuous increment in shear stresses was observed beyond peak stresses in residual region for normal loads of 100 and 200 kPa. The trend shear stresses for normal loads of 300 kPa were much different then lower normal loads. There were continuos reductions in shear stresses in the residual region. Figure 22c shows the shear stress plots for interface test between sand bentonite (100 : 10) and GCL (HDPE side) – Test 24C

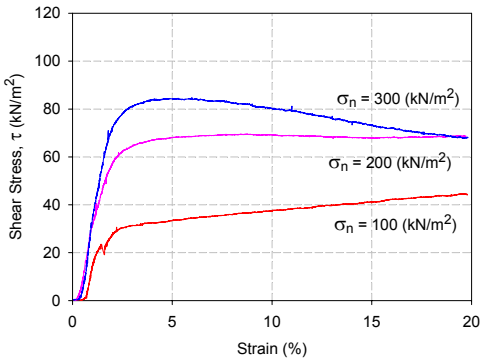

Figure 22c : Test 24C – Sand bentonite (100 : 10) and GCL type 1 (HDPE side), τ (kN/m^2) Vs Strain (%)

Sand bentonite (100 : 10) and GCL type 2 (non woven side) interface, the peak shear stresses were reached within strain of 4 to 8 %. Beyond peak stresses constant residual shear stresses were obtained for all normal loads. Fluctuation in shear stresses in the residual region for normal loads of 200 and 300 kPa were due to tearing of geotextile during the test. Both non woven and woven geotextile were partially to fully torn as the normal loads increase. In all normal stresses there were no peaks or slippage or plowing taking place before peak stresses. Figure 22d shows the shear stress plots for interface test between sand bentonite (100 : 10) and GCL type 2 (non woven side) – Test 25A

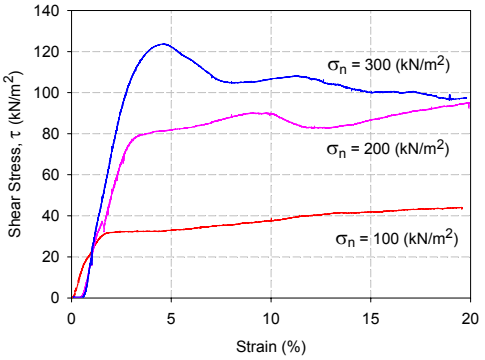

Figure 22d : Test 25A – Sand bentonite (100 : 10) and GCL type 2 (non woven side), τ (kN/m^2) Vs Strain (%)

In the case of sand bentonite (100 : 10) and GCL type 2 (woven side) interface, the peak shear stresses were reached within strain of 6 to 8 %. Partial tearing of woven geotextile took place only of normal loads of 200 and 300 kPa. The pre peaks for 200 and 300 kPa normal loads could be due to tearing of woven geotextile. The trend of interface failure were also similar for 200 and 300 kPa normal loads where beyond peak, reduction in shear stresses occurred before constant residual shear stresses were obtained. For normal load of 100 kPa, heavy plowing force was observed, however the geotextile was not torn, only wavy stress path was observed on woven geotextile. Figure 22e shows the shear stress plots for interface test between sand bentonite (100 : 10) and GCL type 2 (woven side) – Test 25C

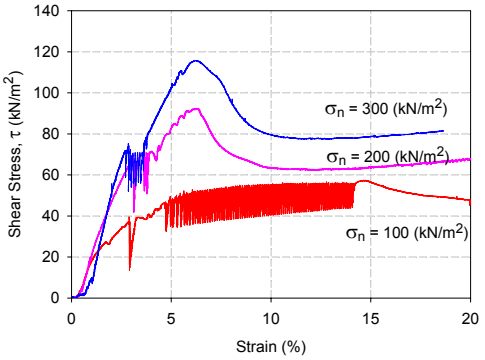

Figure 22e : Test 25C – Sand bentonite (100 : 10) and GCL type 2 (woven side), τ (kN/m^2) Vs Strain (%)

As compared to performance silt bentonite with GCL Type 1 and 2, sand bentonite had better cohesional contribution and with lower frictional

resistance. In general silt bentonite had much better interface properties as compared to sand bentonite. However careful case by case selection is required.

5.8 Native soil interfacing with geosynthetics and compacted clay liner

The performances of native soil with geosynthetics were covered in wide range of friction angle. Only fictional contribution was exhibited without cohesions. The performance of geotextile, HDPE type 1 and PVC (rear side) were the lowest with fiction angle of 15 to 19 degrees. HDPE type 2 provides high frictional resistance. Details of the test results are presented in Table 12 and Figure 23a to 23g respectively.

Table 12 : Test results of native soil interfacing with geosynthetics

Test	Interface Parameters	Cohesion (kN/m²)	Friction Angle (°)
Interface Parameters Between Geosynthetic and Native Soil (HW Granitic Soil)			
TEST 16A	SILT BENTONITE (100 : 10) & NATIVE SOIL	10.3	28.3
TEST 23A	SAND BENTONITE (100 : 10) & NATIVE SOIL	0.0	31.0
TEST 26A	GEOTEXTILE & NATIVE SOIL	0.0	17.8
TEST 27A	HDPE TYPE 1 & NATIVE SOIL	0.0	15.6
TEST 28A	HDPE TYPE 2 & NATIVE SOIL	0.0	23.1
TEST 29A	PVC (Rear) & NATIVE SOIL	0.0	18.7

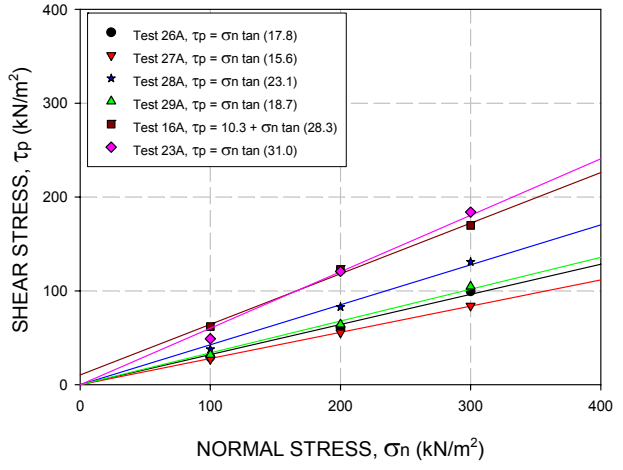

Figure 23a : Summary of peak failure envelopes for native soil interfacing with geosynthetics

For native soil and geotextile interface, the peak shear stresses were reached within strain of 4 to 8 %. Geotextile was ripped apart for normal stresses of 300 kPa. In the case of 100 kPa no damage was observed on the geotextile. Constant shear stresses were observed beyond peak stresses in the residual region. However in the case of normal load of 300 kPa, gradual reduction in shear stresses was observed before constant shear stresses were reached in the residual region. No plowing kind of forces was observed, only minor slippage occurred. Figure 23b shows the shear stress plots for interface test between native soil and geotextile – Test 26A

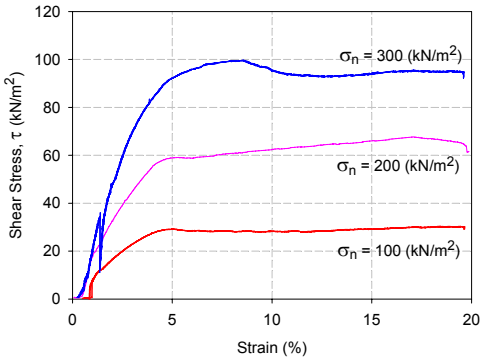

Figure 23b : Test 26A – Native soil and geotextile, τ (kN/m^2) Vs Strain (%)

In the case of interface between native soil and HDPE type 1, the peak shear stresses were reached within strain of 1 to 3 %. Minor reduction of shear stresses was observed beyond peak stresses before constant shear stresses were observed in the residual region. The trends of shear stresses were similar for all tests. No plowing kind of forces was observed, in the tests. Figure 23c shows the shear stress plots for interface test between native soil and HDPE type 1 – Test 27A

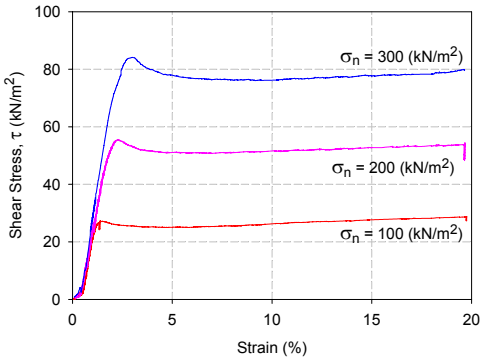

Figure 23c : Test 27A – Native soil and HDPE type 1, τ (kN/m^2) Vs Strain (%)

Interface between native soil and HDPE type 2, the peak shear stresses were reached within strain of 7 to 8 %. The surface of HDPE type 2 was partially to fully sheared during the test depending to the normal loads. Constant shear stresses were

observed beyond peak stresses in the residual region. However in the case of normal load of 300 kPa, gradual reduction in shear stresses was observed before constant shear stresses were reached in the residual region. Minor pre peak and plowing kind of forces were observed. Figure 23d shows the shear stress plots for interface test between native soil and HDPE type 2 – Test 28A

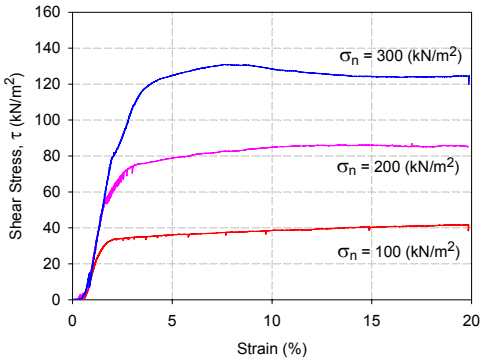

Figure 23d : Test 28A – Native soil and HDPE type 2, τ (kN/m^2) Vs Strain (%)

For interface between native soil and PVC (rear side), the peak shear stresses were reached within strain of 3 to 5.5 %. No damage was observed on the PVC surface. Constant shear stresses were observed beyond peak stresses in the residual region. However in the case of normal load of 300 kPa, gradual reduction in shear stresses was observed before constant shear stresses were reached in the residual region. Minor pre peak and plowing kind of forces were observed. Figure 23e shows the shear stress plots for interface test between native soil and PVC (rear side) – Test 29A

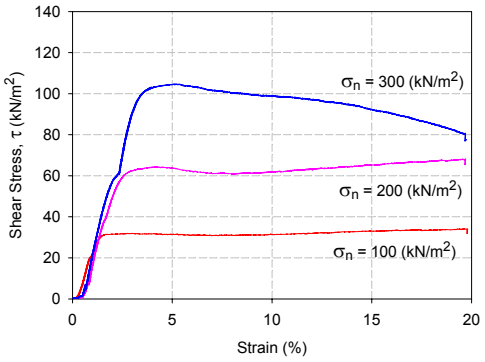

Figure 23e : Test 29A – Native soil and PVC (rear side), τ (kN/m^2) Vs Strain (%))

Interface between native soil and silt bentonite mixture (100 : 10), the peak forces were reached within strain of 7 to 8%. Constant residual shear stresses were observed in the residual region for all normal loads, beyond 6% strain. No plowing kind of effect was observed. Good surface contact was obtained and the failure plane intrudes or cut more into silt bentonite as compared to native soil. Figure 23f shows the shear stress plots for interface test between native soil and silt bentonite (100 : 10) – Test 16A

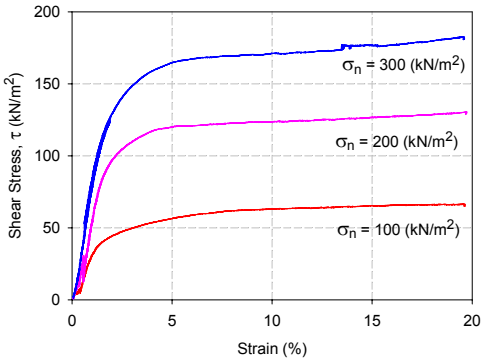

Figure 23f : Test 16A – Native soil and Silt Bentonite (100 : 10), τ (kN/m^2) Vs Strain (%)

In the case of native soil and sand bentonite mixture the peak forces were reached within strain of 7 to 8%. Constant increments in residual shear stresses were observed in the residual region. No plowing kind of effect was observed. Good surface contact was obtained and the failure plane intrude or cut more into native soil as compare to sand bentonite Figure 23g shows the shear stress plots for interface test between native soil and sand bentonite (100 : 10) – Test 23A

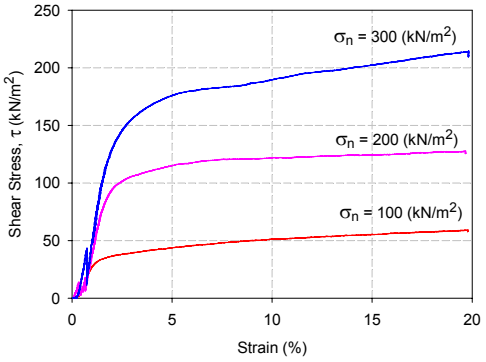

Figure 23g : Test 23A – Native soil and Sand Bentonite (100 : 10), τ (kN/m^2) Vs Strain (%)

The interface properties with native soil exhibits only frictional resistance except for silt bentonite.

Table 13 : Summary of test results

Interfacing Member	Geotextile		HDPE Type 1		HDPE Type 2		PVC (rear side)		PVC (front side)		Native Soil		GCL Type 1 (bentonite side)		GCL Type 1 (HDPE side)		GCL Type 2 (Non Woven Site)		GCL Type 2 (Woven Site)	
	C kN/m²	ϕ 0	C kN/m²	ϕ 0	C kN/m²	ϕ 0	C kN/m²	ϕ 0	C kN/m²	ϕ 0	C kN/m²	ϕ 0	C kN/m²	ϕ 0	C kN/m²	ϕ 0	C kN/m²	ϕ 0	C kN/m²	ϕ 0
HDPE Type 1	0.0	7.6																		
HDPE Type 2	3.2	21.1																		
PVC (rear side)	11.1	18.7																		
PVC (front side)	25.7	17.1																		
GCL Type 1 (bentonite side)	12.1	17.1	0.0	9.1	28.8	19.0	17.6	18.1	0.0	26.3										
GCL Type 1 (HDPE side)	0.0	21.8	2.2	8.9	0.0	19.9	12.1	20.0	0.0	25.2										
GCL Type 2 (Non Woven Site)	1.5	15.1	2.2	7.8	10.2	25.7	17.2	15.3	10.0	17.4										
GCL Type 2 (Woven Site)	10.5	14.8	2.4	9.3	2.1	23.2	14.7	18.1	24.0	18.4										
Silt Bentonite (100 : 10)	0.0	15.3	0.0	15.4	0.0	24.2	0.0	22.2	0.0	20.0	10.3	28.3	13.9	17.0	0.0	22.6	6.2	20.8	1.4	21.4
Sand Bentonite (100 : 10)	0.0	15.8	0.0	13.8	0.0	24.5	0.0	19.8	0.0	16.9	0.0	31	6.5	17.6	14.7	13.7	0.0	22.6	25.7	17.1
Native Soil	0.0	17.8	0.0	15.6	0.0	23.1	0.0	18.7												

The soil and soil (CCLs) interface frictional resistance is about 30 ~ 45 percent lower than average internal friction angle (ϕ) resistance of interfacing soil. The summary of test results are tabulated under table 13.

6 RESULT AND DISCUSSION

Selection of landfill liner depends mainly on environmental protection regulation of individual countries focusing on protection against leachate leakage. However in the geotechnical aspect, selections depend on fill height, interface properties and strain compatibility. As such 9 type of commonly used landfill liner configuration were studied for the interface performances

6.1 Single membrane liner configuration 1 (SMLC 1)

For single liner component it is best to use textured HDPE rather than the usage of smooth surface HDPE. However PVC could contribute in the case of geomembrane for cover soil. For low fill height, cohesion contribution is crucial to provide sufficient FOS. The configuration of direct placement of geomembrane on native soil, requires careful care against microscopic puncture with sufficient sacrificial thickness. Details of the configuration and test results are shown in Figure 4a and Table 2a respectively.

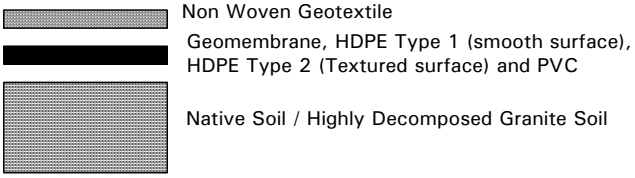

Figure 4a : Single membrane liner configuration 1

Table 2a : Liner configurations and interface tests for single membrane liner configuration 1 (SMLC 1)

Liner Configuration	Interface Test	Description	Interface Parameter	
			Cohesion (kN/m²)	Friction Angle (O)
SMLC 1A	Test 1A	Geotextile & HDPE Type 1	0.0	7.6
	Test 27A	HDPE Type 1 & Native soil	0.0	15.6
SMLC 1B	Test 2A	Geotextile & HDPE Type 2	3.2	21.1
	Test 28A	HDPE Type 2 & Native soil	0.0	23.1
SMLC 1C	Test 3C	Geotextile & PVC (Front Side)	25.7	17.1
	Test 29A	PVC (Rear) & Native soil	0.0	18.7

6.2 Single membrane liner configuration 2 (SMLC 2)

The case of liner configuration 2, is commonly used single liner configuration, where geomembranes are sandwiched between geotextiles. The interface parameters are listed in table 2b. PVC

configuration SMLC 2C had much unified and homogenous frictional contribution as compared to SMLC 2B using HDPE Type 2. Even though HDPE Type 2 had higher frictional resistance, interface between geotextile and native soil is lower. Peak stresses were reached within strain of 4 to 5% for test 2A as compared to strain of 4 to 8% for test 26A. This contributes to strain incompatibility between the member components of liner configuration SMLC 2B. In the case of SMLC 2C, the configuration had reliable strain compatibility, the peak stresses were reached with strain of 4 to 6% for Test 3A, 4 ~7 % for Test 3C and 4 to 8% for Test 26A. The usage of PVC as bottom liner membrane has not been favorite among engineers due to leaching problem of PVC. However it is proposed to use much softer HDPE in order to have sufficient strain compatibility with other members. Details of the configuration and test results are shown in Figure 4b and Table 2b respectively.

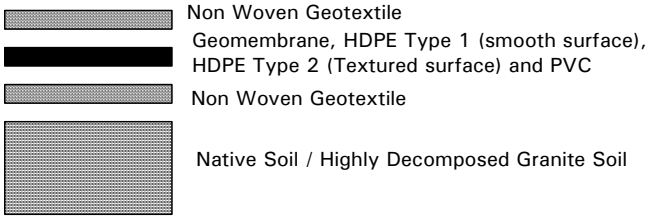

Figure 4b : Single membrane liner configuration 2

Table 2b : Liner configurations and interface tests for single membrane liner configuration 2 (SMLC 2)

Liner Configuration	Interface Test	Description	Interface Parameter	
			Cohesion (kN/m^2)	Friction Angle (^{O})
SMLC 2A	Test 1A	Geotextile & HDPE Type 1	0.0	7.6
	Test 26A	Geotextile & Native soil	0.0	17.8
SMLC 2B	Test 2A	Geotextile & HDPE Type 2	3.2	21.1
	Test 26A	Geotextile & Native soil	0.0	17.8
SMLC 2C	Test 3C	Geotextile & PVC (Front Side)	25.7	17.1
	Test 3A	Geotextile & PVC (Rear Side)	11.1	18.7
	Test 26A	Geotextile & Native soil	0.0	17.8

6.3 Single composite liner configuration 1 (SCLC 1)

In the case of single composite liner configuration 1, where the geomembranes are placed on compacted clay liner, it is found that HDPE Type 2 performed well with both silt and sand compacted as clay liner. The configuration of direct placement of geomembrane on native soil, requires careful care against microscopic puncture with sufficient sacrificial thickness. Both silt and sand had compatible strain with HDPE Type 2 and native soil with strain of 5 ~8%. In the case of PVC, configuration SCLC 1C, SLCL 1D, SCLC 1G and SCLC 1H, both sides of PVC performed well with geotextile and CCLs. There is not much different with in the method of PVC being placed in the liner configuration. Details of the configuration and test results are shown in Figure 4c and Table 2c respectively.

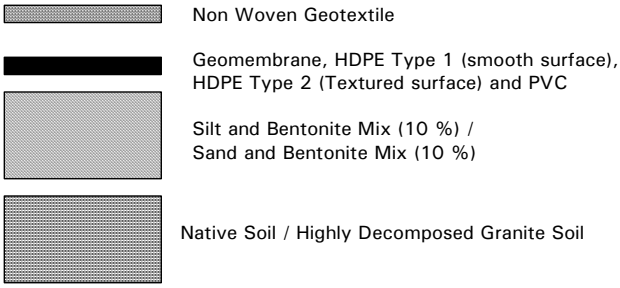

Figure 4c : Single composite liner configuration 1

Table 2c : Liner configurations and interface tests for single composite liner configuration 1 (SCLC 1)

Liner Configuration	Interface Test	Description	Interface Parameter	
			Cohesion (kN/m^2)	Friction Angle (^{O})
SCLC 1A	Test 1A	Geotextile & HDPE Type 1	0.0	7.6
	Test 13A	HDPE Type 1 & Silt Bentonite (100 : 10)	0.0	15.4
	Test 16A	Native soil & Silt Bentonite (100 : 10)	10.3	28.3
SCLC 1B	Test 2A	Geotextile & HDPE Type 2	3.2	21.1
	Test 14A	HDPE Type 2 & Silt Bentonite (100 : 10)	0.0	24.2
	Test 16A	Native soil & Silt Bentonite (100 : 10)	10.3	28.3
SCLC 1C	Test 3C	Geotextile & PVC (Front Side)	25.7	17.1
	Test 15A	PVC (Rear Side) & Silt Bentonite (100 : 10)	0.0	22.2
	Test 16A	Native soil & Silt Bentonite (100 : 10)	10.3	28.3
SCLC 1D	Test 3A	Geotextile & PVC (Rear Side)	11.1	18.7
	Test 15C	PVC (Front Side) & Silt Bentonite (100 : 10)	0.0	20.0
	Test 16A	Native soil & Silt Bentonite (100 : 10)	10.3	28.3
SCLC 1E	Test 1A	Geotextile & HDPE Type 1	0.0	7.6
	Test 13A	HDPE Type 1 & Sand Bentonite (100 : 10)	0.0	13.8
	Test 23A	Native soil & Sand Bentonite (100 : 10)	0.0	31.0
SCLC 1F	Test 2A	Geotextile & HDPE Type 2	3.2	21.1
	Test 21A	HDPE Type 2 & Sand Bentonite (100 : 10)	0.0	24.5
	Test 23A	Native soil & Sand Bentonite (100 : 10)	0.0	31.0
SCLC 1G	Test 3C	Geotextile & PVC (Front Side)	25.7	17.1
	Test 22A	PVC (Rear Side) & Sand Bentonite (100 : 10)	0.0	19.8
	Test 23A	Native soil & Sand Bentonite (100 : 10)	0.0	31.0
SCLC 1H	Test 3A	Geotextile & PVC (Rear Side)	11.1	18.7
	Test 22C	PVC (Front Side) & Sand Bentonite (100 : 10)	0.0	16.9
	Test 23A	Native soil & Sand Bentonite (100 : 10)	0.0	31.0

6.4 Single composite liner configuration 2 (SCLC 2)

In the case of single composite liner configuration 2, where the geomembranes are placed on GCL Type 1 it is found that HDPE Type 2 performed well with both sides of GCL Type 1. Higher cohesion was obtained on bentonite side interfacing with HDPE type 2. In the case of PVC under configuration SCLC 2E and SCLC 2F, higher fictional resistant was obtained for configuration SCLC 2F. As for strain compatibility both Test 4C and 10E reached peak stresses within strain of 4 ~ 6% and 3 ~ 4%. PVC under configuration SCLC 2F could provide high and reliable interface resistance. The configuration of direct placement of geomembrane on GCL Type 1, requires careful care against microscopic puncture with sufficient sacrificial thickness. Details of the configuration and test results are shown in Figure 4d and Table 2d respectively.

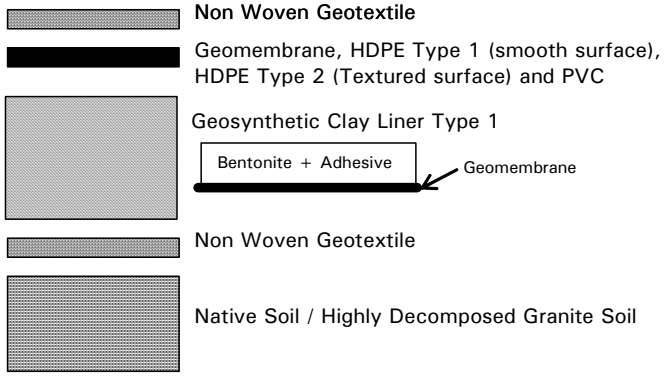

Figure 4d : Single composite liner configuration 2

6.5 Single composite liner configuration 3 (SCLC 3)

For the case of single composite liner configuration 3, where the geomembranes are placed on GCL Type 2 it is found that HDPE Type 2 performed well, however geotextile interfacing with GCL Type 2 and native soil were low. PVC in the case of SCLC 3E had much unified frictional and cohesional resistance and it could contribute to reliable resistance against interface failure. In this configuration both geomembrane and GCL were well protected by geotextiles of both woven and non woven type against microscopic puncture. Details of the configuration and test results are shown in Figure 4e and Table 2e respectively.

Table 2d : Liner configurations and interface tests for single composite liner configuration 2 (SCLC 2)

Liner Configuration	Interface Test	Description	Interface Parameter	
			Cohesion (kN/m^2)	Friction Angle (^{O})
SCLC 2A	Test 1A	Geotextile & HDPE Type 1	0.0	7.6
	Test 6A	HDPE Type 1 & GCL Type 1 (Bentonite Side)	0.0	9.1
	Test 4C	Geotextile & GCL Type 1 (HDPE Side)	0.0	21.8
	Test 26A	Geotextile & Native soil	0.0	17.8
SCLC 2B	Test 1A	Geotextile & HDPE Type 1	0.0	7.6
	Test 6C	HDPE Type 1 & GCL Type 1 (HDPE Side)	2.2	8.9
	Test 4A	Geotextile & GCL Type 1 (Bentonite Side)	12.1	17.1
	Test 26A	Geotextile & Native soil	0.0	17.8
SCLC 2C	Test 2A	Geotextile & HDPE Type 2	3.2	21.1
	Test 8A	HDPE Type 2 & GCL Type 1 (Bentonite Side)	28.8	19.0
	Test 4C	Geotextile & GCL Type 1 (HDPE Side)	0.0	21.8
	Test 26A	Geotextile & Native soil	0.0	17.8
SCLC 2D	Test 2A	Geotextile & HDPE Type 2	3.2	21.1
	Test 8C	HDPE Type 2 & GCL Type 1 (HDPE Side)	0.0	19.9
	Test 4A	Geotextile & GCL Type 1 (Bentonite Side)	12.1	17.1
	Test 26A	Geotextile & Native soil	0.0	17.8
SCLC 2E	Test 3C	Goetextile & PVC (Front Side)	25.7	17.1
	Test 10A	PVC (Rear Side) & GCL Type 1 (Bentonite Side)	17.6	18.1
	Test 4C	Geotextile & GCL Type 1 (HDPE Side)	0.0	21.8
	Test 26A	Geotextile & Native soil	0.0	17.8
SCLC 2F	Test 3A	Goetextile & PVC (Rear Side)	11.1	18.7
	Test 10E	PVC (Front Side) & GCL Type 1 (Bentonite Side)	0.0	26.3
	Test 4C	Geotextile & GCL Type 1 (HDPE Side)	0.0	21.8
	Test 26A	Geotextile & Native soil	0.0	17.8

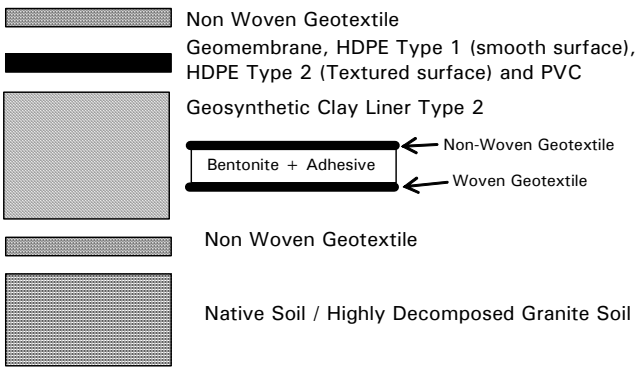

Figure 4e : Single composite liner configuration 3

Table 2e : Liner configurations and interface tests for single composite liner configuration 3 (SCLC 3)

Liner Configuration	Interface Test	Description	Interface Parameter	
			Cohesion (kN/m^2)	Friction Angle (^{O})
SCLC 3A	Test 1A	Geotextile & HDPE Type 1	0.0	7.6
	Test 7A	HDPE Type 1 & GCL Type 2 (Non Woven Site)	2.2	7.8
	Test 5C	Geotextile & GCL Type 2 (Woven Side)	10.5	14.8
	Test 26A	Geotextile & Native soil	0.0	17.8
SCLC 3B	Test 1A	Geotextile & HDPE Type 1	0.0	7.6
	Test 7C	HDPE Type 1 & GCL Type 2 (Woven Side)	2.4	9.3
	Test 5A	Geotextile & GCL Type 2 (Non Woven Site)	1.5	15.1
	Test 26A	Geotextile & Native soil	0.0	17.8
SCLC 3C	Test 2A	Geotextile & HDPE Type 2	3.2	21.1
	Test 9C	HDPE Type 2 & GCL Type 2 (Woven Side)	2.1	23.2
	Test 5A	Geotextile & GCL Type 2 (Non Woven Site)	1.5	15.1
	Test 26A	Geotextile & Native soil	0.0	17.8
SCLC 3D	Test 2A	Geotextile & HDPE Type 2	3.2	21.1
	Test 9A	HDPE Type 2 & GCL Type 2 (Non Woven Side)	10.2	25.7
	Test 5C	Geotextile & GCL Type 2 (Woven Side)	10.5	14.8
	Test 26A	Geotextile & Native soil	0.0	17.8
SCLC 3E	Test 3C	Goetextile & PVC (Front Side)	25.7	17.1
	Test 11A	PVC (Rear Side) & GCL Type 2 (Non Woven Side)	17.2	15.3
	Test 5C	Geotextile & GCL Type 2 (Woven Side)	10.5	14.8
	Test 26A	Geotextile & Native soil	0.0	17.8
SCLC 3F	Test 3A	Goetextile & PVC (Rear Side)	11.1	18.7
	Test 11E	PVC (Front Side) & GCL Type 2 (Non Woven Side)	10.0	17.4
	Test 5C	Geotextile & GCL Type 2 (Woven Side)	10.5	14.8
	Test 26A	Geotextile & Native soil	0.0	17.8
SCLC 3G	Test 3C	Goetextile & PVC (Front Side)	25.7	17.1
	Test 11C	PVC (Rear Side) & GCL Type 2 (Woven Side)	14.7	18.1
	Test 5A	Geotextile & GCL Type 2 (Non Woven Side)	1.5	15.1
	Test 26A	Geotextile & Native soil	0.0	17.8
SCLC 3H	Test 3A	Goetextile & PVC (Rear Side)	11.1	18.7
	Test 11G	PVC (Front Side) & GCL Type 2 (Woven Side)	24.0	18.4
	Test 5A	Geotextile & GCL Type 2 (Non Woven Side)	1.5	15.1
	Test 26A	Geotextile & Native soil	0.0	17.8

6.6 Single composite liner configuration 4 (SCLC 4)

For the case of single composite liner configuration 4, where the geomembranes are sandwiched between CCL of sand bentonite mixture (100 : 10), HDPE Type 2 had high frictional resistance. PCV had narrowly distributed frictional resistance between 17^0 ~20^0 making the probability of potential interface failure occurring either between geotextile with CCL or CCL with PVC. HDPE is preferred choice for this configuration as the probability of failure to occurs is high between geotextile and CCL (Test 19A). The configuration of direct placement of geomembrane on CCL, requires careful care against microscopic puncture with sufficient sacrificial thickness. From all the interface test results using sand bentonite mixture as CCL, the damage to geomembrane and geotextile were very significant. Hence providing sufficient sacrificial thickness is crucial. Details of the configuration and test results are shown in Figure 4f and Table 2f respectively.

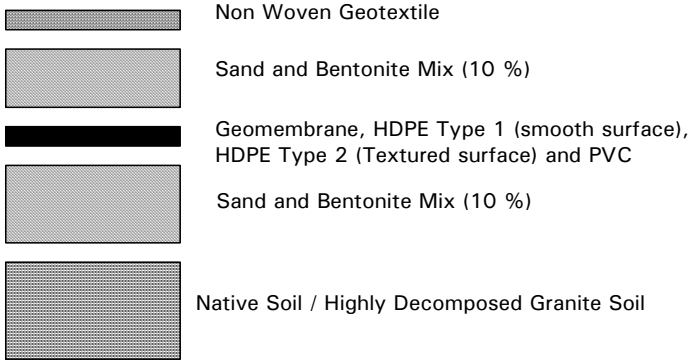

Figure 4f : Single composite liner configuration 4

Table 2f : Liner configurations and interface tests for single composite liner configuration 4 (SCLC 4)

Liner Configuration	Interface Test	Description	Interface Parameter	
			Cohesion (kN/m^2)	Friction Angle (^{O})
SCLC 4A	Test 19A	Geotextile & Sand Bentonite (100 : 10)	0.0	15.8
	Test 20A	HDPE Type 1 & Sand Bentonite (100 : 10)	0.0	13.8
	Test 23A	Native soil & Sand Bentonite (100 : 10)	0.0	31.0
SCLC 4B	Test 19A	Geotextile & Sand Bentonite (100 : 10)	0.0	15.8
	Test 21A	HDPE Type 2 & Sand Bentonite (100 : 10)	0.0	24.5
	Test 23A	Native soil & Sand Bentonite (100 : 10)	0.0	31.0
SCLC 4C	Test 19A	Geotextile & Sand Bentonite (100 : 10)	0.0	15.8
	Test 22C	PVC (Front Side) & Sand Bentonite (100 : 10)	0.0	16.9
	Test 22A	PVC (Rear Side) & Sand Bentonite (100 : 10)	0.0	19.8
	Test 23A	Native soil & Sand Bentonite (100 : 10)	0.0	31.0
SCLC 4D	Test 19A	Geotextile & Sand Bentonite (100 : 10)	0.0	15.8
	Test 22A	PVC (Rear Side) & Sand Bentonite (100 : 10)	0.0	19.8
	Test 22C	PVC (Front Side) & Sand Bentonite (100 : 10)	0.0	16.9
	Test 23A	Native soil & Sand Bentonite (100 : 10)	0.0	31.0

6.7 Single composite liner configuration 5 (SCLC 5)

The interface trend of single composite liner configuration 5 is similar to those of liner configuration 4, where HDPE Type 2 had high frictional resistance with silt bentonite mixture (100 : 10). PVC frictional resistance with silt bentonite mixture was higher as compared to sand bentonite mixture. PVC had narrowly distributed frictional resistance between 20^0 ~22^0 , higher by 2^0 ~3^0, making the probability of potential interface failure occurring either between geotextile with CCL or CCL with PVC. HDPE is preferred choice for this configuration as the probability of failure to occurs is high between geotextile and CCL (Test 12A). The configuration of direct placement of geomembrane on CCL, requires careful care against microscopic puncture with sufficient sacrificial thickness. The damage created by silt bentonite mixture was lower as compared to damages created by sand bentonite mixture to geomembrane and geotextile. Details of the configuration and test results are shown in Figure 4g and Table 2g respectively.

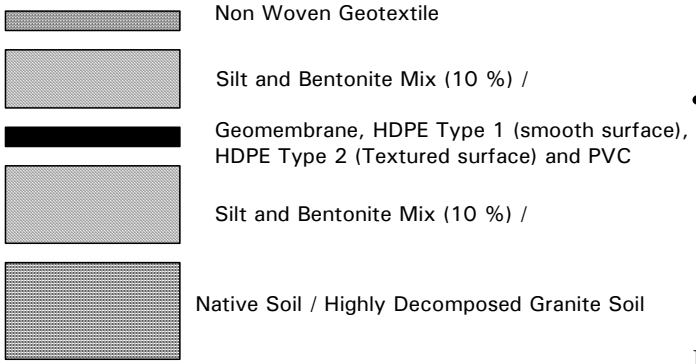

Figure 4g : Single composite liner configuration 5

6.8 Single composite liner configuration 6 and 7 (SCLC 6 and 7)

For the single composite liner configuration 6 and 7 with sandwiches GCL Type 1 between silt bentonite mixture (configuration 6) and sand bentonite mixture (configutation 7). There is not much variation in the interface performance, both had similar frictional resistance. However silt bentonite mixture had higher frictional resistance when interfaced with HDPE side of GCL Type 1. Probability the usage of silt bentonite mixture will be a better choice as CCL. Details of the configuration and test results are shown in Figure 4h and 4i and Table 2h and 2i respectively.

Table 2g : Liner configurations and interface tests for single composite liner configuration 5 (SCLC 5)

Liner Configuration	Interface Test	Description	Interface Parameter	
			Cohesion (kN/m^2)	Friction Angle (^{O})
SCLC 5A	Test 12A	Geotextile & Silt Bentonite (100 : 10)	0.0	15.3
	Test 13A	HDPE Type 1 & Silt Bentonite (100 : 10)	0.0	15.4
	Test 16A	Native soil & Silt Bentonite (100 : 10)	10.3	28.3
SCLC 5B	Test 12A	Geotextile & Silt Bentonite (100 : 10)	0.0	15.3
	Test 14A	HDPE Type 2 & Silt Bentonite (100 : 10)	0.0	24.2
	Test 16A	Native soil & Silt Bentonite (100 : 10)	10.3	28.3
SCLC 5C	Test 12A	Geotextile & Silt Bentonite (100 : 10)	0.0	15.3
	Test 15C	PVC (Front Side) & Silt Bentonite (100 : 10)	0.0	20.0
	Test 15A	PVC (Rear Side) & Silt Bentonite (100 : 10)	0.0	22.2
	Test 16A	Native soil & Silt Bentonite (100 : 10)	10.3	28.3
SCLC 5D	Test 12A	Geotextile & Silt Bentonite (100 : 10)	0.0	15.3
	Test 15A	PVC (Rear Side) & Silt Bentonite (100 : 10)	0.0	22.2
	Test 15C	PVC (Front Side) & Silt Bentonite (100 : 10)	0.0	20.0
	Test 16A	Native soil & Silt Bentonite (100 : 10)	10.3	28.3

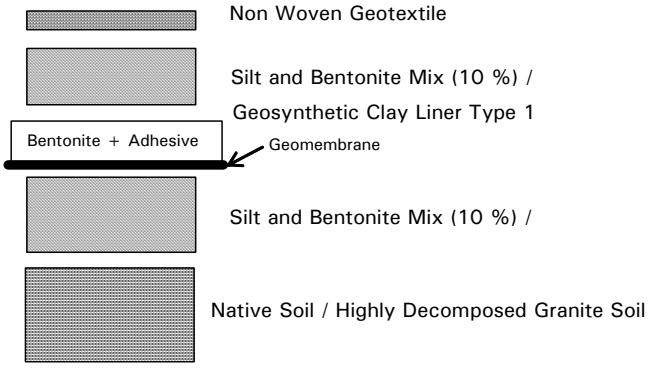

Figure 4h : Single composite liner configuration 6

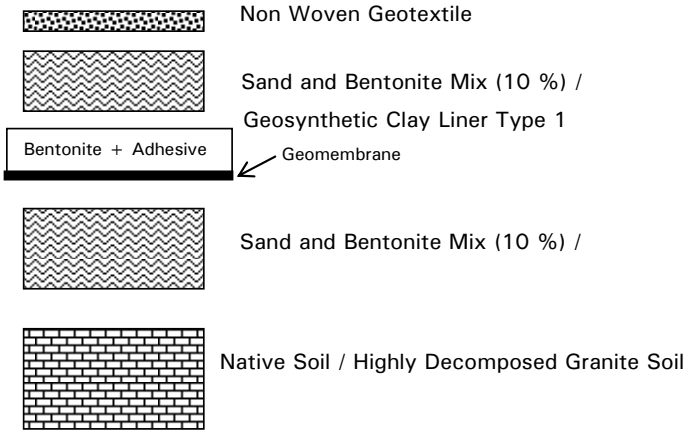

Figure 4i : Single composite liner configuration 7

Table 2h : Liner configurations and interface tests for single composite liner configuration 6 (SCLC 6)

Liner Configuration	Interface Test	Description	Interface Parameter	
			Cohesion (kN/m^2)	Friction Angle (^{O})
SCLC 6A	Test 12A	Geotextile & Silt Bentonite (100 : 10)	0.0	15.3
	Test 17A	GCL Type 1 (Bentonite Side) & Silt Bentonite (100 : 10)	13.9	17.0
	Test 17C	GCL Type 1 (HDPE Side) & Silt Bentonite (100 : 10)	0.0	22.6
	Test 16A	Native soil & Silt Bentonite (100 : 10)	10.3	28.3
SCLC 6B	Test 12A	Geotextile & Silt Bentonite (100 : 10)	0.0	15.3
	Test 17C	GCL Type 1 (HDPE Side) & Silt Bentonite (100 : 10)	0.0	22.6
	Test 17A	GCL Type 1 (Bentonite Side) & Silt Bentonite (100 : 10)	13.9	17.0
	Test 16A	Native soil & Silt Bentonite (100 : 10)	10.3	28.3

Table 2i : Liner configurations and interface tests for single composite liner configuration 7 (SCLC 7)

Liner Configuration	Interface Test	Description	Interface Parameter	
			Cohesion (kN/m^2)	Friction Angle (^{O})
SCLC 8A	Test 19A	Geotextile & Sand Bentonite (100 : 10)	0.0	15.8
	Test 24A	GCL Type 1 (Bentonite Side) & Sand Bentonite (100 : 10)	6.5	17.6
	Test 24C	GCL Type 1 (HDPE Side) & Sand Bentonite (100 : 10)	14.7	13.7
	Test 23A	Native soil & Sand Bentonite (100 : 10)	0.0	31.0
SCLC 8B	Test 19A	Geotextile & Sand Bentonite (100 : 10)	0.0	15.8
	Test 24C	GCL Type 1 (HDPE Side) & Sand Bentonite (100 : 10)	14.7	13.7
	Test 24A	GCL Type 1 (Bentonite Side) & Sand Bentonite (100 : 10)	6.5	17.6
	Test 23A	Native soil & Sand Bentonite (100 : 10)	0.0	31.0

6.9 Single composite liner configuration 8 and 9 (SCLC 8 and 9)

For the single composite liner configuration 8 and 9 with sandwiches GCL Type 2 between silt bentonite mixture (configuration 8) and sand bentonite mixture (configutation 9). There is not much variation in the interface performance, both had similar frictional resistance. However silt bentonite mixture had overall higher frictional resistance when interfaced with GCL Type 2. Even though sand bentonite mixture had higher frictional resistance with non woven side of GCL Type 2, it had lower resistance for woven side of GCL Type 2. In the case of silt bentonite mixture both sides of GCL Type 2 contributed to similar fictional resistance. Hence the liner configuration with silt bentonite mixture could perform as unified member pushing the probability of interface failure to geotextile (Test 12A). Details of the configuration and test results are shown in Figure 4j and 4k and Table 2j and 2k respectively.

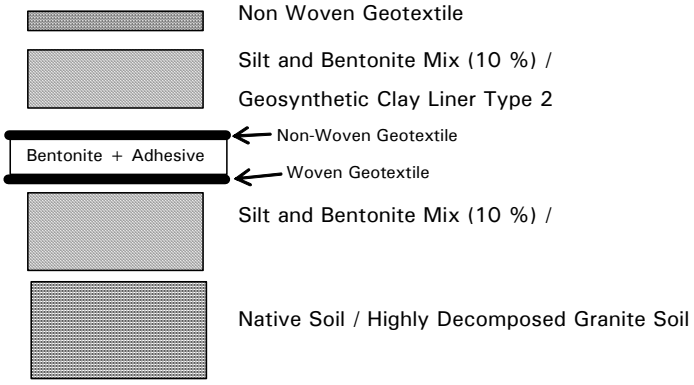

Figure 4j : Single composite liner configuration 7

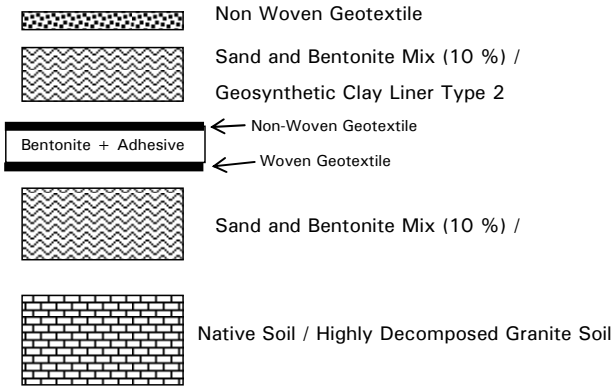

Figure 4k : Single composite liner configuration 9

Table 2j : Liner configurations and interface tests for single composite liner configuration 7 (SCLC 7)

Liner Configuration	Interface Test	Description	Interface Parameter	
			Cohesion (kN/m^2)	Friction Angle (^{O})
SCLC 7A	Test 12A	Geotextile & Silt Bentonite (100 : 10)	0.0	15.3
	Test 18A	GCL Type 2 (Non Woven Side) & Silt Bentonite (100 : 10)	6.3	20.8
	Test 18C	GCL Type 2 (Woven Side) & Silt Bentonite (100 : 10)	1.4	21.4
	Test 16A	Native soil & Silt Bentonite (100 : 10)	10.3	28.3
SCLC 7B	Test 12A	Geotextile & Silt Bentonite (100 : 10)	0.0	15.3
	Test 18C	GCL Type 2 (Woven Side) & Silt Bentonite (100 : 10)	1.4	21.4
	Test 18A	GCL Type 2 (Non Woven Side) & Silt Bentonite (100 : 10)	6.3	20.8
	Test 16A	Native soil & Silt Bentonite (100 : 10)	10.3	28.3

Table 2k : Liner configurations and interface tests for single composite liner configuration 9 (SCLC 9)

Liner Configuration	Interface Test	Description	Interface Parameter	
			Cohesion (kN/m^2)	Friction Angle (^{O})
SCLC 9A	Test 19A	Geotextile & Sand Bentonite (100 : 10)	0.0	15.8
	Test 25A	GCL Type 2 (Non Woven Side) & Sand Bentonite (100 : 10)	0.0	22.6
	Test 25C	GCL Type 2 (Woven Side) & Sand Bentonite (100 : 10)	25.8	17.1
	Test 23A	Native soil & Sand Bentonite (100 : 10)	0.0	31.0
SCLC 9B	Test 19A	Geotextile & Sand Bentonite (100 : 10)	0.0	15.8
	Test 25C	GCL Type 2 (Woven Side) & Sand Bentonite (100 : 10)	25.8	17.1
	Test 25A	GCL Type 2 (Non Woven Side) & Sand Bentonite (100 : 10)	0.0	22.6
	Test 23A	Native soil & Sand Bentonite (100 : 10)	0.0	31.0

8 REFERENCES

ASTM D3080–98 “Standard Test Method for Direct Shear Test of Soils Under Consolidated Drained Conditions”. Annual Book of ASTM Standards, Vol 04.08. pp 347 – 352.

ASTM D5321–02 “Standard Test Method for Determining the Coefficient of Soil and Geosynthetic or Geosynthetic and Geosynthetic Friction by the Direct Shear Method”. Annual Book of ASTM Standards, Vol 04.13. pp 123-129.

ASTM D6243–98 “Standard Test Method for Determining the Internal and Interface Shear Resistance of Geosynthetic Clay Liner by the Direct Shear Method”. Annual Book of ASTM Standards, Vol 04.13. pp 287-293.

David E. Daniel, Robert M. Koerner, Rudolph Bonaparte, Robert E. Landreth, David A. Carson and Heather B. Scranton (July 1998) “Slope Stability Of Geosynthetic Clay Liner test Plots”, Journal of Geotechnical and Geoenvironmental Engineering, pp 628-637.

Eric J. Triplett and Patrick J. Fox (June 2001) “Shear Strength of HDPE Geomembrane / Geosynthetic Clay Liner Interfaces”, Journal of Geotechnical and Geoenvironmental Engineering, pp 543-552.

Hiroshi Obana, (Jan 2000) “Resources Reduction Through Ecocement Production”, 2nd CTI / Industry Joint Seminar : Technology in Asia, 14 - 15 January 2000 Cebu City, Philippines.

Hisham T. Eid, Timothy D. Stark, W. Douglas Evans, and Paul E. Sherry (May 2000) “Municipal Solid Waste Slope Failure. I Waste and Foundation Soil Properties”, Journal of Geotechnical and Geoenvironmental Engineering, pp 397-407.

Hoe I. Ling and Dov Leshchinsky, (February 1997) “Seismic Stability And Permanent Displacement of Landfill Cover Systems”, Journal of Geotechnical and Geoenvironmental Engineering, pp 113-122.

Joseph E. Dove, P.E., and J. David Frost, P.E., (July 1999) “Peak Friction Behavior of Smooth Geomembrane-Particle Interfaces”, Journal of Geotechnical and Geoenvironmental Engineering, pp 544-555.

Kamon, M (1989) “Definition of Environmental Geotechnology” Proc. 2nd ICSMFE, Rio de Janeiro, 5: 3126-3130.

Kamon, M and Jang, Y.-S. (2001) “Solution Scenarios of Geo-Environmental Problems”, Eleventh Asian Regional Conference on Soil Mechanics and Geotechnical Engineering”. S. W. Hong et al., Swets & Zeitlinger, Lisse, pp. 833-852.

Kamon, M. and Katsumi, T. (2001): Clay liners for waste landfill, Clay Science for Engineering”, K. Adachi and M. Fukue, eds., Balkema, Rotterdam, pp. 29-45.

Koerner, R. M. and Soong, T. (2000b). “Stability assessment of ten large landfill failures”, Advances in Transportation and Geoenvironment Systems Using Geosynthetics, Geotechnical Special Publication No. 103, J.G. Zornberg and B.R. Christopher (Eds.), ASCE, pp 1-38.

Patrick J. Fox, Michael G. Rowland, and John R. Scheithe, (October 1998) “Internal Shear Strength of Three Goesynthetic Clay Liners”, Journal of Geotechnical and Geoenvironmental Engineering, pp 933-944.

Robert B. Gilbert, Stephen G Wright, and Eric Liedtke (Dec 1998) “Uncertainty in Back Analysis of Slopes : Kettleman Hills Case History”, Journal of Geotechnical and Geoenvironmental Engineering, pp 1167-1176.

Timothy D. Stark, Hisham T. Eid, W. Douglas Evans and Paul E. Sherry (May 2000) “Municipal Solid Waste Slope Failure. II Stability Analyses”, Journal of Geotechnical and Geoenvironmental Engineering, pp 408-419.

Wenxing Jian (Sept 2001) “Evaluation of Landfill Stability Relating to Clay Liners”, Report of Postdoctoral Research.

Xuede Qian, Robert M. Koerner and Donald H. Gray, (2002), “Geotechnical Aspects of Landfill Design and Construction”, Prentice Hall.

Xuede Qian, Robert M. Koerner and Donald H. Gray, (June 2003) “Translational Failure Analysis of Landfills”, Journal of Geotechnical and Geoenvironmental Engineering, pp 506-519.